CONTRACTOR REPORT

SAND82-7120
Unlimited Release
UC-63c

Design and Demonstration of a Spectrum-Splitting Photovoltaic Concentrator Module

P. G. Borden, P. E. Gregory, O. E. Moore
Varian Associates, Inc.
Solid State Laboratory
611 Hansen Way
Palo Alto, CA 94303

Prepared by Sandia National Laboratories Albuquerque, New Mexico 87185 and Livermore, California 94550 for the United States Department of Energy under Contract DE-AC04-76DP00789

Printed November 1982

When printing a copy of any digitized SAND Report, you are required to update the markings to current standards.

Issued by Sandia National Laboratories, operated for the United States Department of Energy by Sandia Corporation.

NOTICE: This report was prepared as an account of work sponsored by an agency of the United States Government. Neither the United States Government nor any agency thereof, nor any of their employees, nor any of their contractors, subcontractors, or their employees, makes any warranty, express or implied, or assumes any legal liability or responsibility for the accuracy, completeness, or usefulness of any information, apparatus, product, or process disclosed, or represents that its use would not infringe privately owned rights. Reference herein to any specific commercial product, process, or service by trade name, trademark, manufacturer, or otherwise, does not necessarily constitute or imply its endorsement, recommendation, or favoring by the United States Government, any agency thereof or any of their contractors or subcontractors. The views and opinions expressed herein do not necessarily state or reflect those of the United States Government, any agency thereof or any of their contractors or subcontractors.

Printed in the United States of America
Available from
National Technical Information Service
U.S. Department of Commerce
5285 Port Royal Road
Springfield, VA 22161

NTIS price codes
Printed copy: A04
Microfiche copy: A01

SAND82–7120
Unlimited Release
Printed November 1982

Distribution
Category UC–63c

Design and Demonstration of a Spectrum-Splitting Photovoltaic Concentrator Module

P. G. Borden, P. E. Gregory, O. E. Moore
Varian Associates, Inc.
Solid State Laboratory
611 Hansen Way
Palo Alto, CA 94303

Contract No. 13–0308

Abstract

Varian Associates, Inc. has designed and fabricated a spectrum splitting, concentrating photovoltaic module that uses point focus curved facet Fresnel lenses to concentrate incident sunlight. The concentrated sunlight beam spectrum is split into a high and low energy part by a dichroic filter. The high energy part of the spectrum is transmitted to an AlGaAs solar cell and the low energy part is reflected to a Si cell. Spectrum splitting and using cells that respond best to the two parts of the spectrum gives a higher efficiency than the use of either cell alone.

Varian has tested their experimental module, which consists of 10 AlGaAs and 10 Si cells, and has measured a sunlight to electricity conversion efficiency of 20%.

TABLE OF CONTENTS

Section		Page
I.	INTRODUCTION	1
II.	MODULE STRUCTURE	2
III.	OPTICS	8
	A. The Fresnel Lens	8
	B. Filters	18
IV.	CELLS	20
	A. The Silicon Cell	20
	B. The AlGaAs Cell	26
V.	MODULE TESTING	32
	A. Cell Alignment	32
	B. Method of Testing	33
	C. Single-Cell Test Results	35
	D. Wiring Configuration for the Module	39
	E. Module Test Results	42
	1. Test Data	42
	2. Comparison to Past Split Spectrum Work	46
VI.	CONCLUSION	54
APPENDIX A:	SUMMARY OF TEST DATA FOR SPECTRAL SPLITTING	56
REFERENCES		61

I. INTRODUCTION

This report describes the design, fabrication, and testing of a dichroic filter spectrum-splitting module. This is the first demonstration of the spectrum-splitting concept at the module level, and has achieved a record module efficiency -- 20.5%.

Spectrum splitting has long been recognized as an attractive means of obtaining high photovoltaic conversion efficiencies. The idea is to break the solar spectrum into different energy components. These components illuminate two or more solar cells, each with a different bandgap. This mode of operation effectively circumvents the design compromise encountered when using a single solar cell -- i.e., a low bandgap is desirable for collecting more photons, but a high bandgap is needed to get a high operating voltage.

The dichroic filter used in this module breaks the spectrum into two components. This filter consists of multiple dielectric layers laid down on a glass substrate. It has a sharp cutoff near the bandgap of the high-bandgap cell, so that high energy light transmits to this cell (made of AlGaAs), while low energy light reflects to a silicon cell. This type of configuration was originally demonstrated in 1978.[1] The present work represents a significant advance in that the concept has been extended to the module level without a sacrifice in efficiency.

This report has five sections. The first describes the mechanical assembly of the module. The second discusses the optical system. The third section presents a description of the solar cells, and the fourth outlines the testing program and the results obtained. Finally, a conclusion summarizes the results and discusses their significance.

II. MODULE STRUCTURE

The module consists of ten concentrator cones mounted on a common I-beam support. This is shown in Fig. II-1. Note that the hexagonal shape of the cones allows close packing; a number of these modules could form an array with a minimal loss of collection area. The acrylic cones fasten to the aluminum support in a manner that anchors them firmly in only one place. This permits relative motion of the plastic and aluminum in the plane of the beam to prevent warping of the assembly due to temperature changes.

This relative motion is accomplished by slotting the holes in the aluminum beam and securing the plastic cone with spring-loaded screws to control frictional drag along the slot, while at the same time preventing vertical motion by a high spring rate in that direction. Spring loading is accomplished by sandwiching a neoprene washer between two steel washers and controlling compression of the neoprene.

Figure II-2 shows an individual cone. The top is closed by an acrylic curved-groove fresnel lens, cemented in place. Chapter III discusses the lens design in detail. It has a hexagonal shape, with a diagonal measure of 8". With an active area of 41.57 square inches, it provides a geometric concentration ratio of 477 suns on a 1/3-inch-diameter cell. The f number, in this case defined as the ratio of focal length to diagonal measure, is 3.8.

The upper body of the cone has a hexagonal shape matched to the size of the lens. This is formed from flat acrylic pieces cemented together. The lower body, also made of acrylic, has a square shape. The interior of the cone is lined with a thin aluminum conical shield, to prevent the beam of concentrated light from damaging the plastic cone during off-track operation. Additional heat shielding is provided with aluminum aperture plates in front of the cell holders.

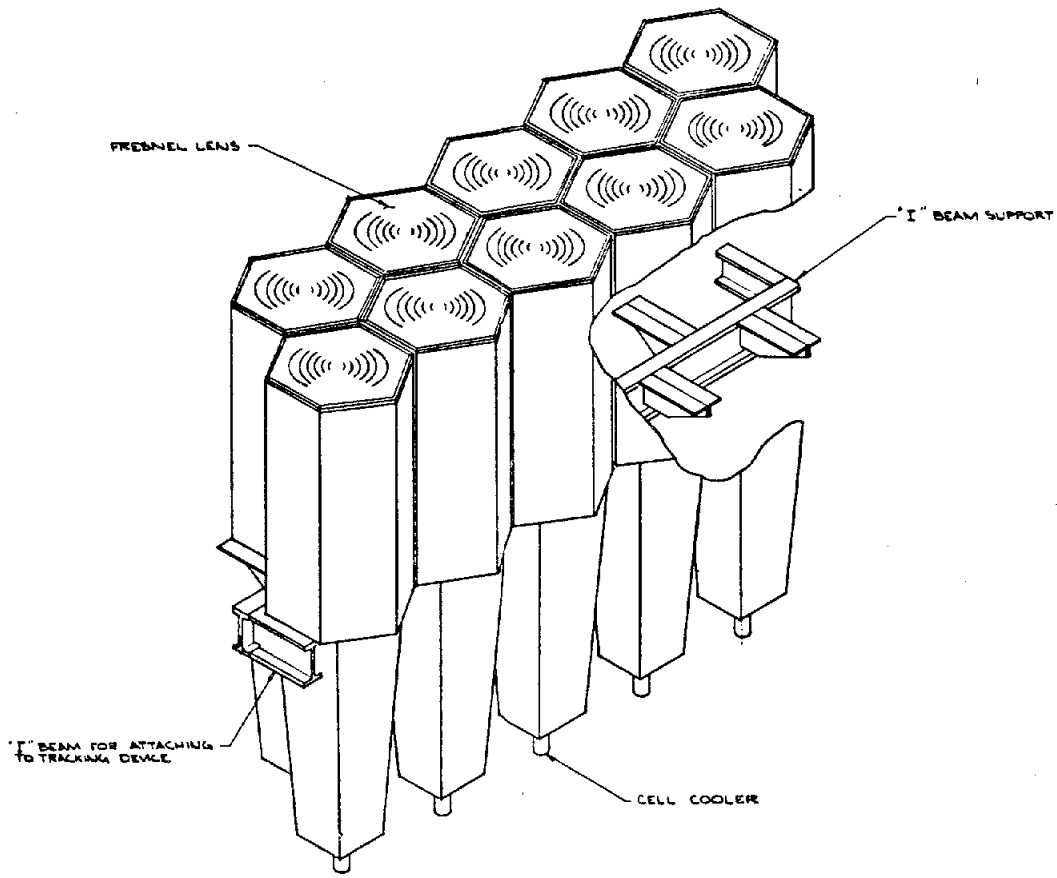

Fig. II-1 Spectrum splitter module.

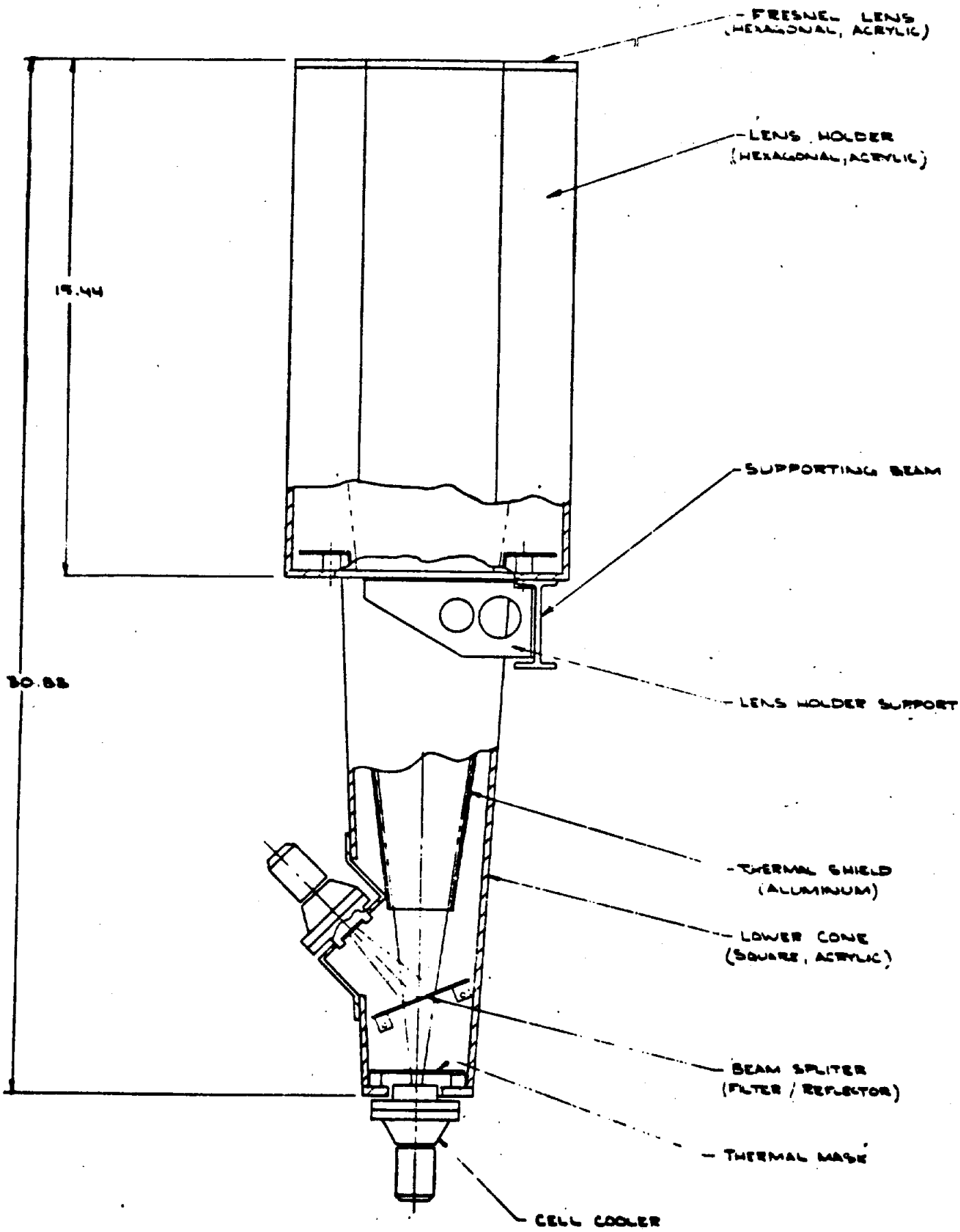

Fig. II-2 An Individual Cone.

The dichroic filter mounts in an aluminum frame 2.75 inches up from the AlGaAs cell. It sits at an angle of 22.5 degrees. This may be adjusted slightly in order to compensate for variations in the construction of the cones.

A packaged cell, designed to fit into the jet impingement holder, appears in Fig. II-3.* The cells themselves are described in Sec. IV. The same packaging process was used for both HBG and LBG cells. The package consists of 60-mil thick Al-300 alumina. The metal pattern is fired-in molymanganese, with a Ni-Ag plating. Copper lead tabs, brazed on, carry out the current.

The cell is vacuum soldered to the alumina baseplate with a Sn-3%Ag solder. Contact to the top is made with a silver-plated copper leadframe. The leadframe contacts the top of the cell die at each of the die's four corners, through use of a Pb-In paste. The entire assembly is thus fabricated in a two-step process, whereby the cell die is first soldered to the baseplate and the leadframe then soldered to the corners of the cell die.

The cells mount in plastic jet-impingement coolers, as shown in Fig. II-3. These were originally designed to be a low-cost molded part, and are similar to those made for an earlier Sandia contract (ET-78-C-04- 5313), with a slightly smaller nozzle diameter to allow for the smaller diameter of the active area and the lower level of insolation on each cell. The silicon cells mount in coolers made of PVC plastic; the AlGaAs cells mount in Ryton coolers. PVC was selected for the silicon cells because they are not expected to operate at high temperatures, owing to their high coefficient of efficiency loss with respect to temperature. The service temperature of PVC is about 65°C, and it is a relatively low-

---

*The cell shown in the figure has a .49" diameter active area on a 1/2" square substrate. The cells used in the module had a 1/3" diameter active area on the same size substrate, fitting into the same package.

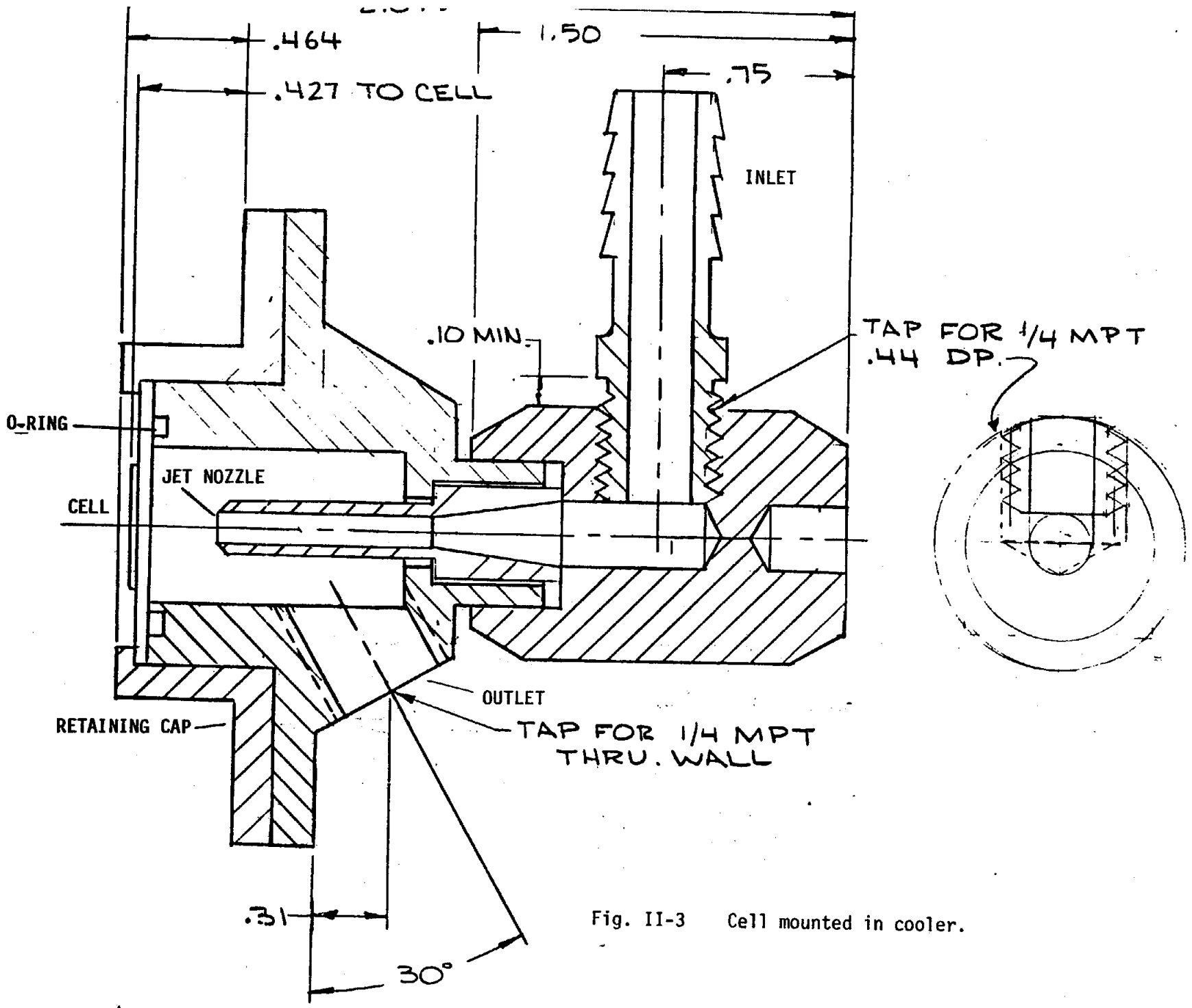

Fig. II-3 Cell mounted in cooler.

III. OPTICS

This section discusses the spectral splitter's optics system. The principal components are the curved-groove fresnel lens and the spectral-splitting filter. The design of these and the performance of the actual components are described below.

A. The Fresnel Lens

The fresnel lens was designed with the aid of a Monte Carlo ray-trace computer program. This program takes into account such effects as the finite width of the disc of the sun, dispersion in the lens plastic, and groove draft angle and tip radius. The photon energy range, lens diagonal measure, lens-cell spacing, groove depth, cell design diameter and edge step width are defined by the user. The program then generates a facet table and, by drawing a specified number of rays from the sun to the cell, plots the radial intensity distribution in the plane of the cell.

Initially, both long and short focal length systems were considered. The layouts are shown in Fig. III-1. In the long focal length system, the filter is mounted at an angle. Light reflects to the low-bandgap cell, which is mounted to the side of the beam. In the short focal length system, the filter is not tilted and the cell receiving reflected light sits in the optical path. This added obscuration and the larger filter size would tend to outweigh the advantages of a more compact system with less critical alignment tolerances.

Another advantage of the long focal length system is shown in Fig. III-2. This shows both lens-to-cell transmission and the ratio of peak-to-average concentration as a function of lens-cell spacing. A .49" cell and 11.7" diagonal measure lens were assumed. These values were used early in the design, and later changed to the .333" cell and 8"

cost material, so that it is ideal for a cell cooler that should not operate above 50°C. The coolers for the AlGaAs cells are made of Ryton polyphenylene sulfide) in order to allow the cooling water for these cells to go as high as 100°C. This allows for the possibility of some thermal recovery from the high-bandgap cells.

The alumina baseplate packages fit into the holder over an O-ring seal. A cap, held in place with 2 screws, firmly forces the package down onto the O-ring. The copper lead tabs pass uncer this cap to the screws, which fit through holes at the ends of the lead tabs.

The cooling system connects the ten silicon cell holders in one series string and the ten AlGaAs cell holders in another. The two strings connect in parallel. The most efficient flow rate is calculated to be .0624 GPM (3.94×10^{-3} liters/second) through each cooler, or .1248 GPM (7.87×10^{-3} l/s) for the array.

Fig. III-1 POSSIBLE CONFIGURATIONS FOR SPECTRUM SPLITTING

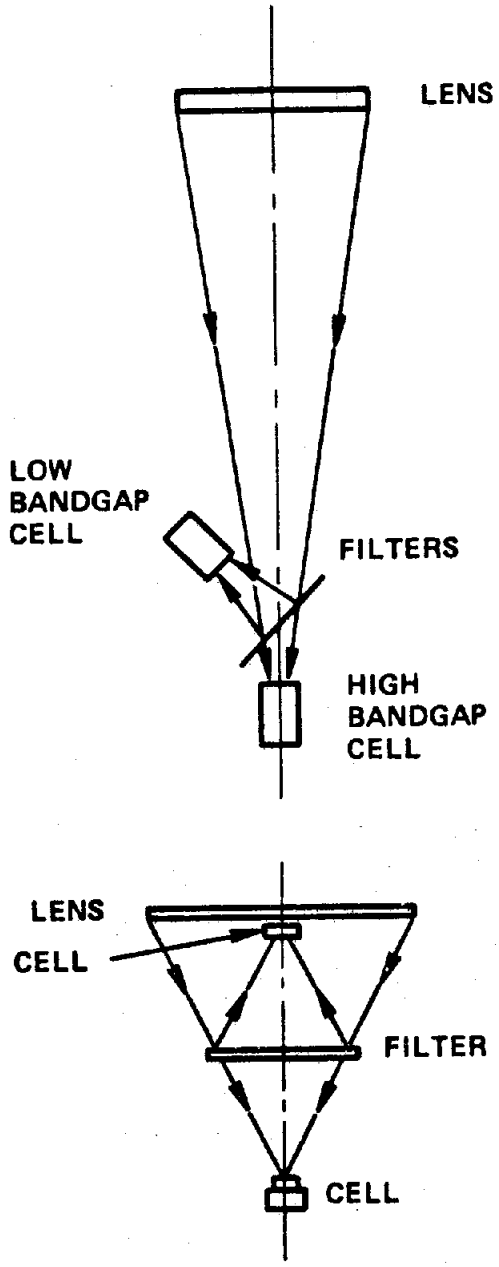

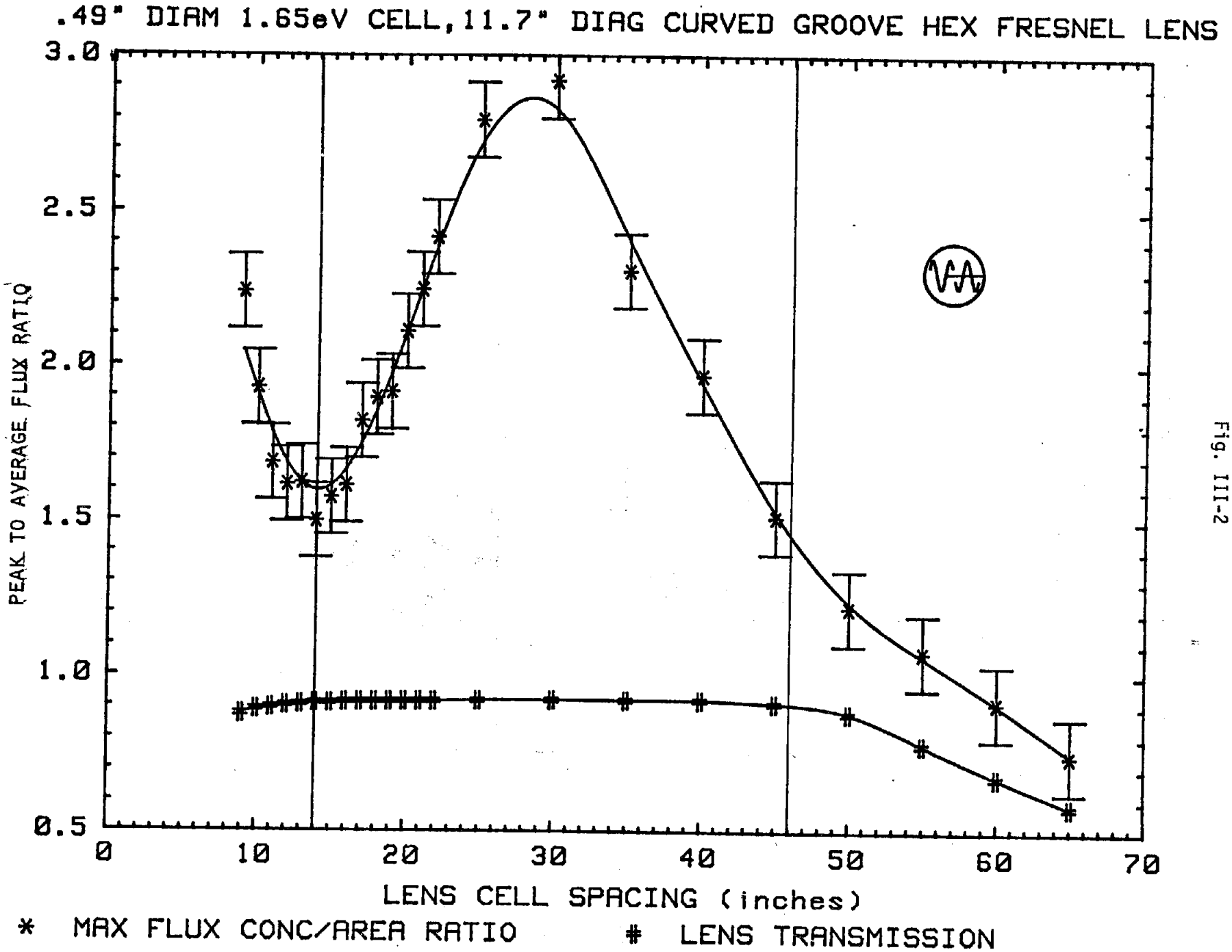
.49" DIAM 1.65eV CELL,11.7" DIAG CURVED GROOVE HEX FRESNEL LENS
PEAK TO AVERAGE FLUX RATIO
3.0
2.5
2.0
1.5
1.0
0.5
0
10
20
30
40
50
60
70
LENS CELL SPACING (inches)
* MAX FLUX CONC/AREA RATIO
# LENS TRANSMISSION

Fig. III-2

diagonal measure actually used. The shape of the curves in Fig. III-2 are the same for both systems, so that conclusions drawn therefrom are identical. It is desirable to minimize the peak-to-average concentration ratio while miantaining high transmission. This maximizes both fill factor and short circuit current, thereby maximizing output power. Note that while the transmission is about the same for short and long focal length systems, the latter has a lower peak-to-average concentration ratio. This, as well as the earlier-mentioned reasons, dictated use of a long focal length design.

The principal drawback to this choice is sensitivity to tracking error. Figure III-3 shows the lens transmission (fraction of light actually hitting the cell) as a function of tracking error. The long focal length system is seen to be much more sensitive, requiring better than ±.1° accuracy. This is about three times more critical than the short focal length system. As was learned in the test phase of the program, this is compounded by the fact that the complexity of the optical system, with two cells, a filter, and a lens, makes it very desirable to allow as much room for alignment and tracking error as possible.

As stated above, the final choice of lens diagonal measure was 8 inches. The focal length was 30.5 inches. The shop drawing of the lens blank is shown in Fig. III-4. The computer input parameters and lens specifications are shown in Fig. III-5. Figure III-6 shows the lens sag table. Figure III-7 shows the predicted radial intensity distribution and Fig. III-8 is a 3-dimensional plot of the same data; these were obtained by Monte Carlo ray tracing.

Sample lenses were delivered. These had imperfections due to diamond tool marks. Optical Sciences Group (OSG, the manufacturer) claims this was due to noise coupling on the single point machine that made the master. As a result, the measured transmission (by laser scan) of the sample lens was 84-85% rather than the anticipated 88-89%.

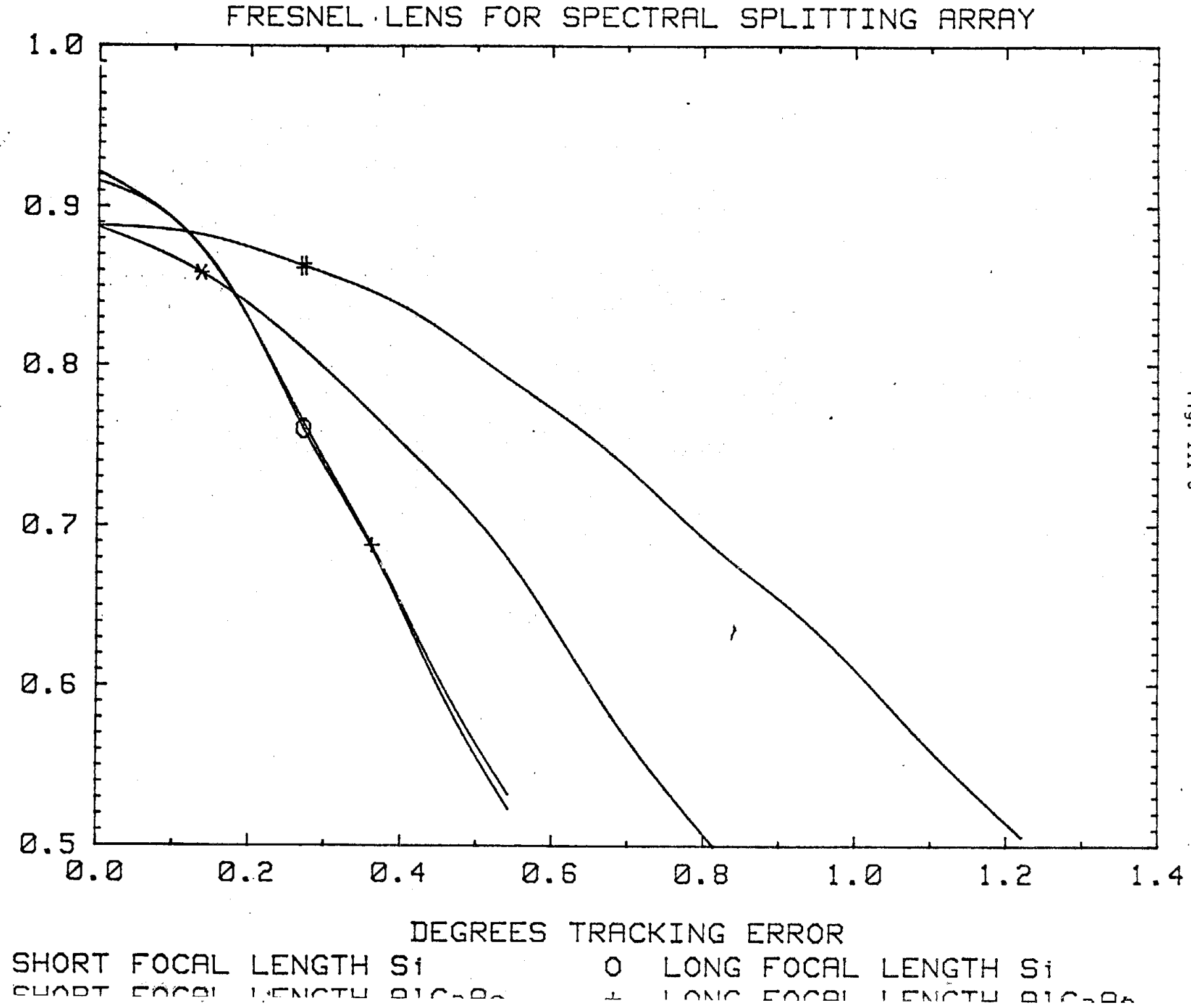
FRESNEL LENS FOR SPECTRAL SPLITTING ARRAY
1.0
0.9
0.8
0.7
0.6
0.5
0.0
0.2
0.4
0.6
0.8
1.0
1.2
1.4
DEGREES TRACKING ERROR
SHORT FOCAL LENGTH Si
O LONG FOCAL LENGTH Si

Fig. III-3

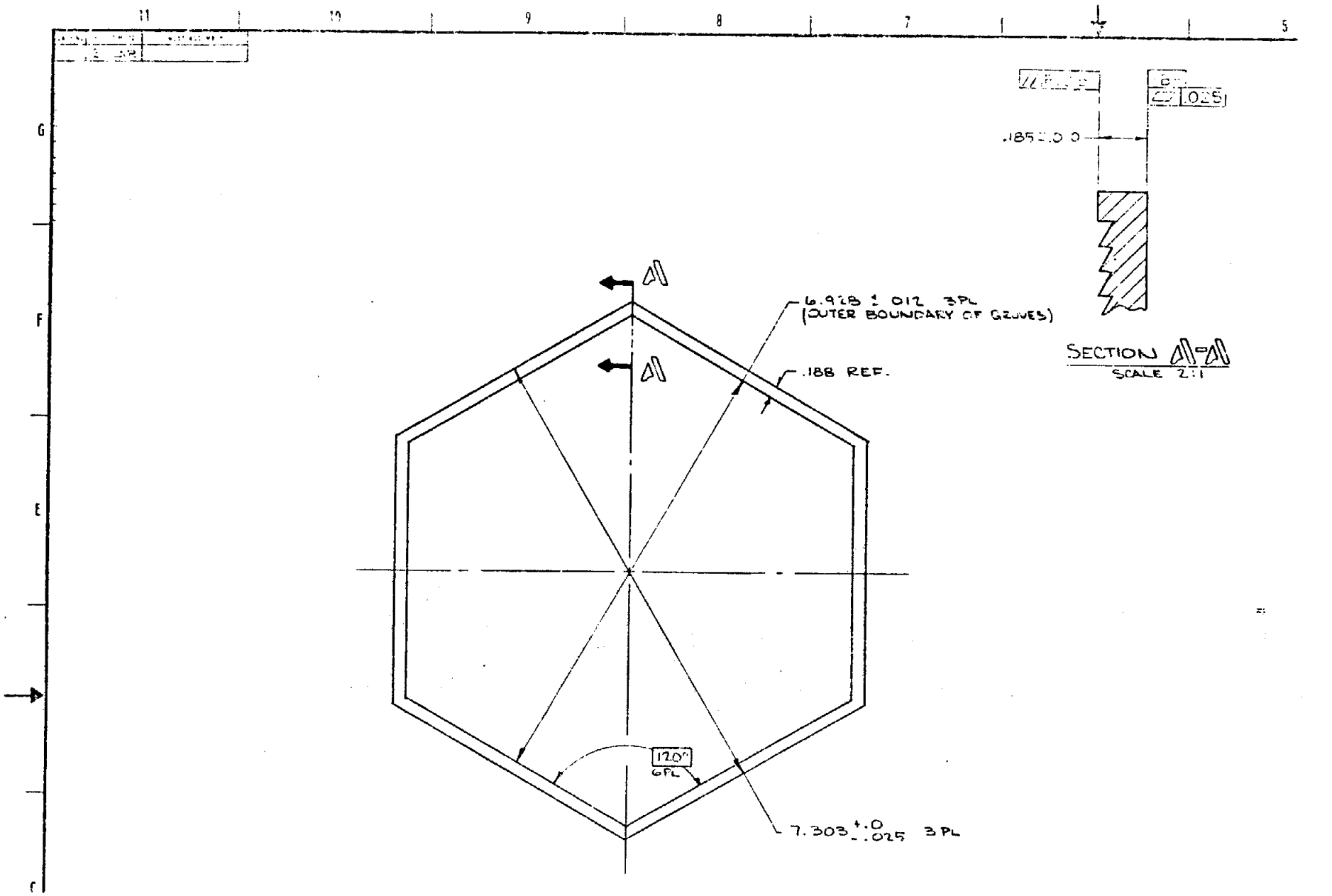

Fig. III-4 Fresnel Lens

Fig. III-5

USER DEFINABLE KEYS
#0 RESTART
#1 CURRENT NUMBER OF RAYS
#8 LENS FACET TABLE
#9 LENS SAG TABLE
#10 EARLY END

AM2 RED EDGE FRESNEL MCRT, HEX APP, CONSTANT DEPTH CURVED GROOVES

LOW hν = 1.65 eV. HIGH hν = 2.8 eV. DESIGN hν = 1.65 eV.
DIAGONAL IS 8 INCHES LONG
CELL 30.5 INCHES BEHIND LENS
GROOVE DEPTH = .06 UNLESS GROOVE WIDTH EXCEEDS 4 INCHES.
EDGE STEP WIDTH IS .2311 INCHES
.2 Deg DRAFT ANGLE
.0001 INCH TIP RADII
MINIMUM CELL DIAMETER = .444 INCHES
CELL DESIGN DIAMETER IS .368 INCHES
-.0175 INCHES EXTRA RADIUS FOR TOLERANCES
CELL DIAMETER = .333 INCHES
MAXIMUM INPUT ANGLE ON CELL = 7.81 Deg
30000 RAYS TO BE TRACED
LENS FACET TABLE
0
2139
2180

CURVED GROOVE FRESNEL LENS SPECS

R = RADIUS FROM THE LENS CENTER
H = HEIGHT FROM THE VALLEY POINTS ON LENS, FROM THE PEAKS ON THE TOOLING

All dimensions given in INCHES, all angles are given in DEGREES.

FACET #	PEAK R	PEAK H	VALLEY R	VALLEY H	RADIUS OF CURVATURE	ANGLE AT INSIDE EDGE
1	0.00000000	0.06	0.03965888	0.06000000	FLAT	0.00000000
2	0.03965888	0.06	1.37090147	-.00000000	14.79839017	0.00000000
3	1.37111091	0.06	1.92380954	-.00000000	15.09067717	5.14020954
4	1.92401898	0.06	2.34914691	-.00000000	15.43843141	7.23660376
5	2.34935635	0.06	2.70853471	-.00000000	15.79856561	8.82322936
6	2.70874415	0.06	3.02585462	0.00000000	16.16808351	10.14233175
7	3.02606406	0.06	3.31335302	-.00000000	16.54589819	11.28844328
8	3.31356247	0.06	3.57830207	-.00000000	16.93150616	12.31036799
9	3.57851151	0.06	3.82543759	-.00000000	17.22465164	13.23728284
10	3.82564703	0.06	4.05804723	-.00000000	17.72520441	14.08831751

SAG TABLE HEIGHT IN INCHES

R+V +	0.000	0.010	0.020	0.030	0.040
0.000	0.0600000000	0.0600000000	0.0600000000	0.0600000000	0.0599999962
0.050	0.0599963870	0.0599960197	0.0599688955	0.0599450138	0.0599143745
0.100	0.0598769776	0.0598329230	0.0597819108	0.0597242407	0.0596598121
0.150	0.0595886262	0.0595106822	0.0594259801	0.0593345197	0.0592363009
0.200	0.0591313235	0.0590195875	0.0589010926	0.0587758381	0.0586438251
0.250	0.0585050527	0.0583595208	0.0582072291	0.0580481775	0.0578823657
0.300	0.0577097936	0.0575304608	0.0573443664	0.0571515116	0.0569518954
0.350	0.0567455175	0.0565323777	0.0563124756	0.0560858110	0.0558523835
0.400	0.0556121928	0.0553652300	0.0551115200	0.0548510376	0.0545837910
0.450	0.0543097794	0.0540290024	0.0537414597	0.0534471510	0.0531460758
0.500	0.0528382331	0.0525236237	0.0522022465	0.0518741012	0.0515391872
0.550	0.0511975042	0.0508490515	0.0504938289	0.0501318356	0.0497630707
0.600	0.0493875350	0.0490052271	0.0486161467	0.0482202932	0.0478176661
0.650	0.0474082647	0.0469920879	0.0465691364	0.0461394090	0.0457029050
0.700	0.0452596240	0.0448095652	0.0443527281	0.0438891120	0.0434187163
0.750	0.0429415397	0.0424575828	0.0419668443	0.0414693236	0.0409650200
0.800	0.0404539327	0.0399360611	0.0394114044	0.0388799619	0.0383417325
0.850	0.0377967161	0.0372449118	0.0366863189	0.0361209362	0.0355487635
0.900	0.0348697996	0.0343840438	0.0338914953	0.0333921525	0.0328860161
0.950	0.0319730846	0.0313535569	0.0307268224	0.0300935102	0.0294533394
1.000	0.0288064689	0.0281527474	0.0274922257	0.0268249010	0.0261507735
1.050	0.0254690414	0.0247821053	0.0240875628	0.0233862133	0.0226780560
1.100	0.0219630890	0.0212413129	0.0205127259	0.0197773271	0.0190351153
1.150	0.0182860896	0.0175302490	0.0167673923	0.0159981179	0.0152218261
1.200	0.0144397150	0.0136487837	0.0128520310	0.0120484557	0.0112380563
1.250	0.0104208333	0.0095967839	0.0087659067	0.0079282021	0.0070836681
1.300	0.0062323032	0.0053741075	0.0045090785	0.0036372154	0.0027585170
1.350	0.0018729320	0.0009806087	0.0000813970	0.0591977316	0.0582888645
1.400	0.0573732980	0.0564510000	0.0555220008	0.0545862876	0.0536438607
1.450	0.0526947174	0.0517388573	0.0507762793	0.0498069918	0.0488309929
1.500	0.0478482223	0.0468587576	0.0458625687	0.0448596537	0.0438500106
1.550	0.0428336392	0.0418105369	0.0407807036	0.0397441367	0.0387008361
1.600	0.0376507990	0.0365940253	0.0355305123	0.0344602600	0.0333832654
1.650	0.0322995286	0.0312090473	0.0301118135	0.0290078450	0.0278971204
1.700	0.0267796471	0.0256554208	0.0245244418	0.0233867072	0.0222422167
1.750	0.0210909676	0.0199329596	0.0187681898	0.0175966580	0.0164183619
1.800	0.0152332992	0.0140414697	0.0128428704	0.0116375010	0.0104253586
1.850	0.0092064429	0.0079807503	0.0067482821	0.0055090337	0.0042630053
1.900	0.0030101938	0.0017505989	0.0004842175	0.0592298514	0.0579622800
1.950	0.0566785716	0.0553882242	0.0540912361	0.0527876051	0.0514773308
2.000	0.0501604107	0.0488368425	0.0475066259	0.0461697533	0.0448262225
2.050	0.0434760629	0.0421152322	0.0407557428	0.0393855945	0.0380087846
2.100	0.0366251109	0.0352351726	0.0338387675	0.0324358924	0.0310264434
2.150	0.0296079315	0.0281944397	0.0267742723	0.0253474270	0.0239139010
2.200	0.0224236940	0.0209668032	0.0195032268	0.0180329622	0.0165560038
2.250	0.0150723640	0.0135820252	0.0120849917	0.0105812600	0.0090708302
2.300	0.0075536989	0.0060298643	0.0044993238	0.0029620767	0.0014181202
2.350	0.0598000761	0.0583441400	0.0568816421	0.0552125803	0.0536369526
2.400	0.0520547571	0.0504659917	0.0488706544	0.0472687433	0.0456602563
2.450	0.0440451913	0.0424235464	0.0407953194	0.0391605084	0.0375191111
2.500	0.0358711257	0.0342165458	0.0325553816	0.0308876188	0.0292132594
2.550	0.0275323011	0.0258447419	0.0241505797	0.0224498123	0.0207424374
2.600	0.0190284530	0.0173078568	0.0155806467	0.0138468205	0.0121063759
2.650	0.0103593108	0.0086056228	0.0068453098	0.0050783695	0.0033047990
2.700	0.0015245974	0.0597752909	0.0579892390	0.0561828998	0.0543769723
2.750	0.0525645536	0.0507456415	0.0489202332	0.0470883277	0.0452499221
2.800	0.0434050135	0.0415536009	0.0396956314	0.0378312528	0.0359603121
2.850	0.0340628583	0.0321988884	0.0303084001	0.0284113205	0.0265078585
2.900	0.0245578011	0.0226812153	0.0207581000	0.0188284522	0.0168922696
2.950	0.0149495491	0.0130002895	0.0110444827	0.0090821413	0.0071132481
3.000	0.0051378057	0.0031558115	0.0011672625	0.0592136504	0.0572120231
3.050	0.0552037839	0.0531891304	0.0511680603	0.0491405705	0.0471066598
3.100	0.0450663253	0.0430195644	0.0409663748	0.0389067534	0.0368406990
3.150	0.0347682085	0.0326892794	0.0306039042	0.0285120955	0.0264138357
3.200	0.0242091263	0.0221979675	0.0200803546	0.0179562855	0.0158257578
3.250	0.0136887683	0.0115453150	0.0093953965	0.0072390086	0.0050761491
3.300	0.0029069155	0.0007310052	0.0585938574	0.0564043636	0.0542085332
3.350	0.0520063631	0.0497978502	0.0475829931	0.0453617887	0.0431342339
3.400	0.0409003272	0.0386600655	0.0364134461	0.0341604660	0.0319011237
3.450	0.0296354160	0.0273633397	0.0250848933	0.0228000736	0.0205088779
3.500	0.0182113031	0.0159073476	0.0135970081	0.0112802814	0.0089571660
3.550	0.0066276586	0.0042917559	0.0019494563	0.0596047862	0.0572533804
3.600	0.0547407133	0.0525617833	0.0501865873	0.0478051219	0.0454173857
3.650	0.0430233755	0.0406230879	0.0382165215	0.0358036730	0.0333845392
3.700	0.0309591134	0.0285274067	0.0260894027	0.0236451030	0.0211945043
3.750	0.0187376050	0.0162744017	0.0138043911	0.0113290716	0.0088469398
3.800	0.0063584924	0.0038637276	0.0013626416	0.0588969682	0.0563915254
3.850	0.0538298951	0.0513428752	0.0488080636	0.0462678568	0.0437214517
3.900	0.0411688459	0.0386100374	0.0360450222	0.0334737986	0.0308963628
3.950	0.0283127130	0.0257223454	0.0231267582	0.0205244475	0.0179159115

Fig. III-6 Sag Table: lens thickness as a function of radius in in inches. Radius read as sum of first column entry plus entry at top of data column.

OPTICS LAYOUT,& INTERSECTION OF RAYS WITH CELL (FACETS 2 TIMES REAL SCALE)

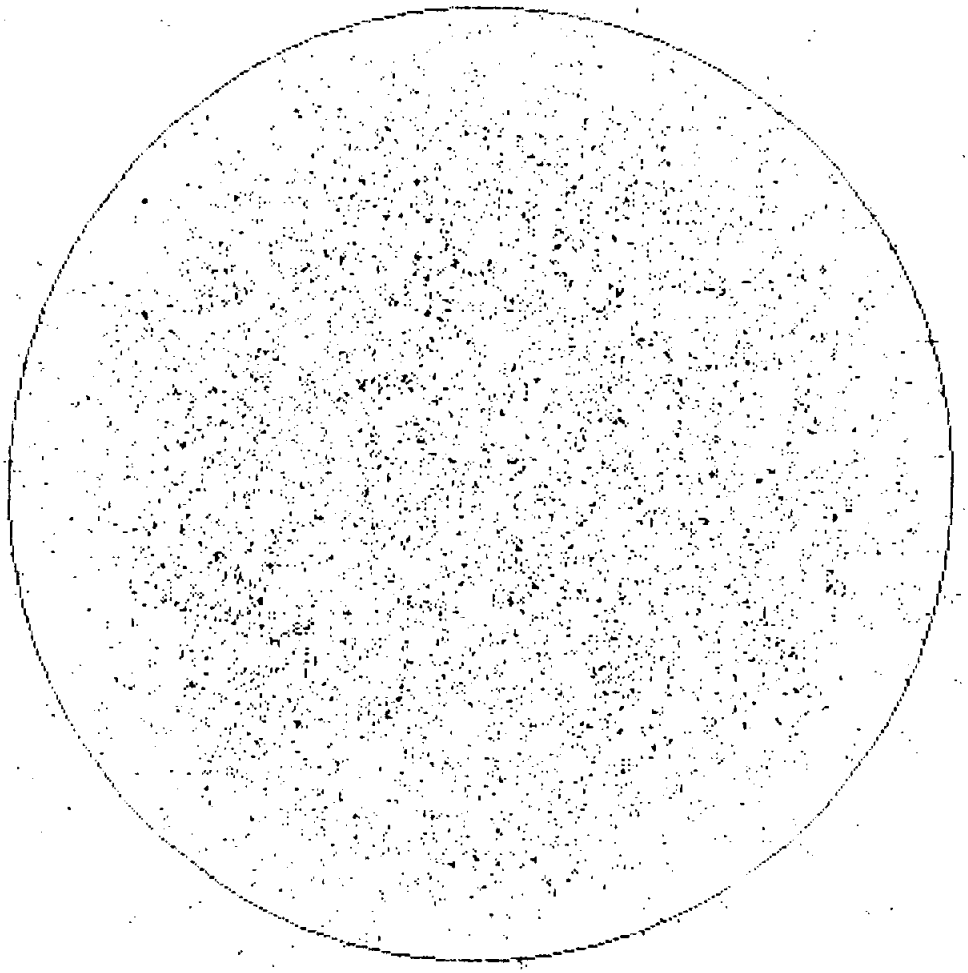

AVERAGE LENS TRANSMISSION = .908
FRACTION OF RAYS LOST IN LENS = .0008
FRACTION OF RAYS THAT MISSED CELL = .0163
RATIO OF MAXIMUM TO AVERAGE CONCENTRATION = 1.584

Fig. III-7 Radial intensity distribution at the high bandgap cell.

Fig. III-8

SPECTRUM SPLITTER FRESNEL LENS:
INTENSITY AS A FUNCTION OF POSITION AT THE SOLAR CELL

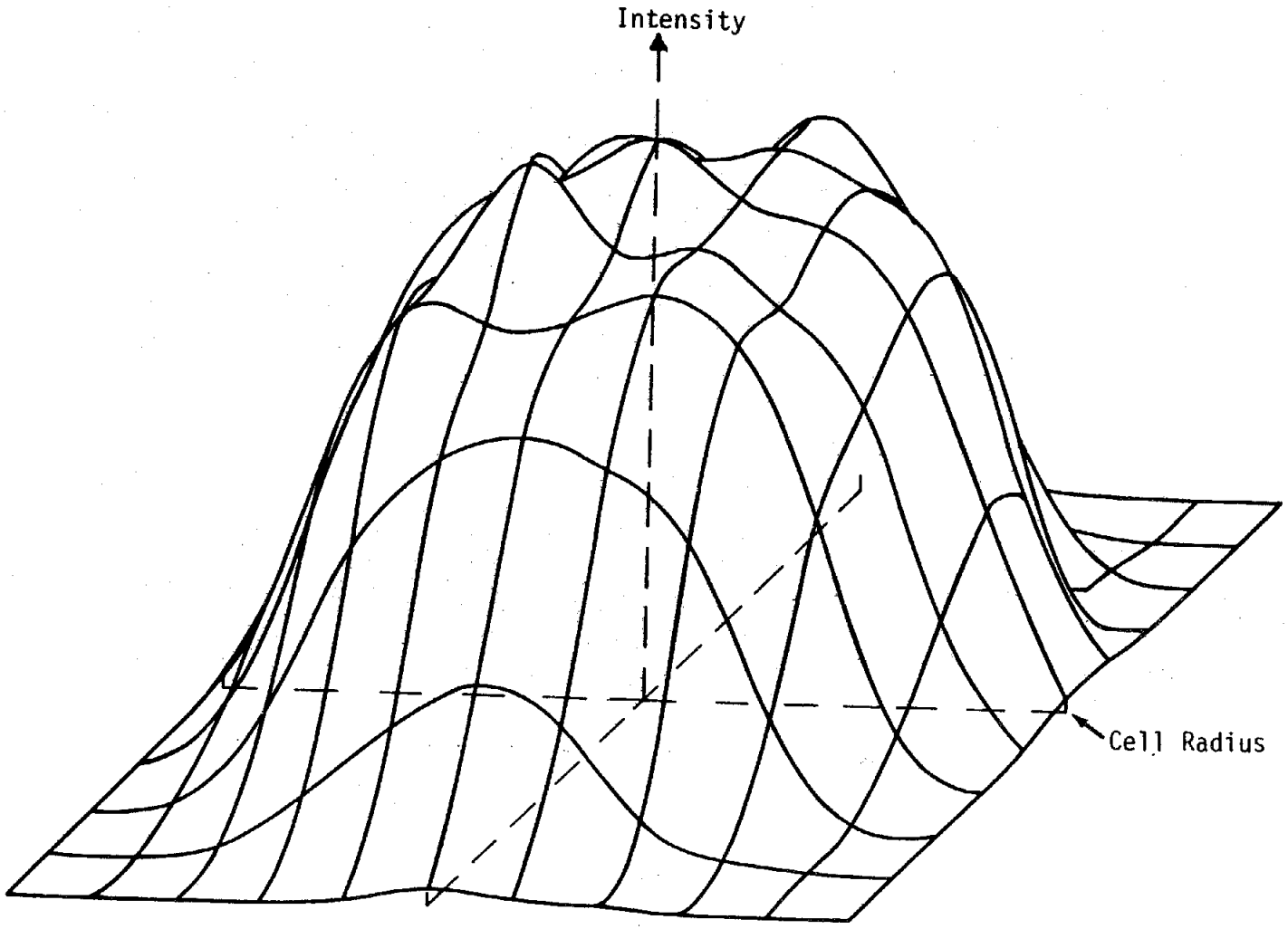

Because of the added cost and the uncertainty as to whether retooling would result in a significant improvement, it was decided to accept these lenses. A more detailed discussion of lens transmission to 1/3"- and 1/2"-diameter cells appears in Sec. V-2.

B. Filters

To optimize performance, it is necessary to have a filter that cuts off sharply at the bandgap energy of the high-bandgap cell, 1.65 eV. Furthermore, sidelobes must be minimized to prevent sending high-energy photons to the silicon cell or low-energy photons to the AlGaAs cell. A multilayer dielectric filter is required to achieve this performance, and considerable design work was carried out under Sandia contract 07-6953. In this contract, 17 layer filters had been designed and fabricated.[2] They had been shown to perform quite acceptably for this application. The drawback was that these filters tended to degrade in humid air, and were thus unacceptable for meeting the 20-year lifetime goal for the optical components.

Rather than continuing the filter development work, it was decided to simply order filters from an outside vendor, OCLI (Optical Coating Labs, Inc.). While the filters received fell within the tolerances specified by the vendor, they are, unfortunately, not ideal for the present application. As can be seen from the transmission characteristics shown in Fig. III-9, these filters (which are of a design and composition proprietary to OCLI) have a cutoff at 1.55 eV rather than the desired 1.65 eV. A good fraction of the light between 1.55 and 1.65 eV is thus transmitted to the AlGaAs cell, where it is of no use in producing electric power. In Sec. V-2, the magnitude of this loss will be calculated.

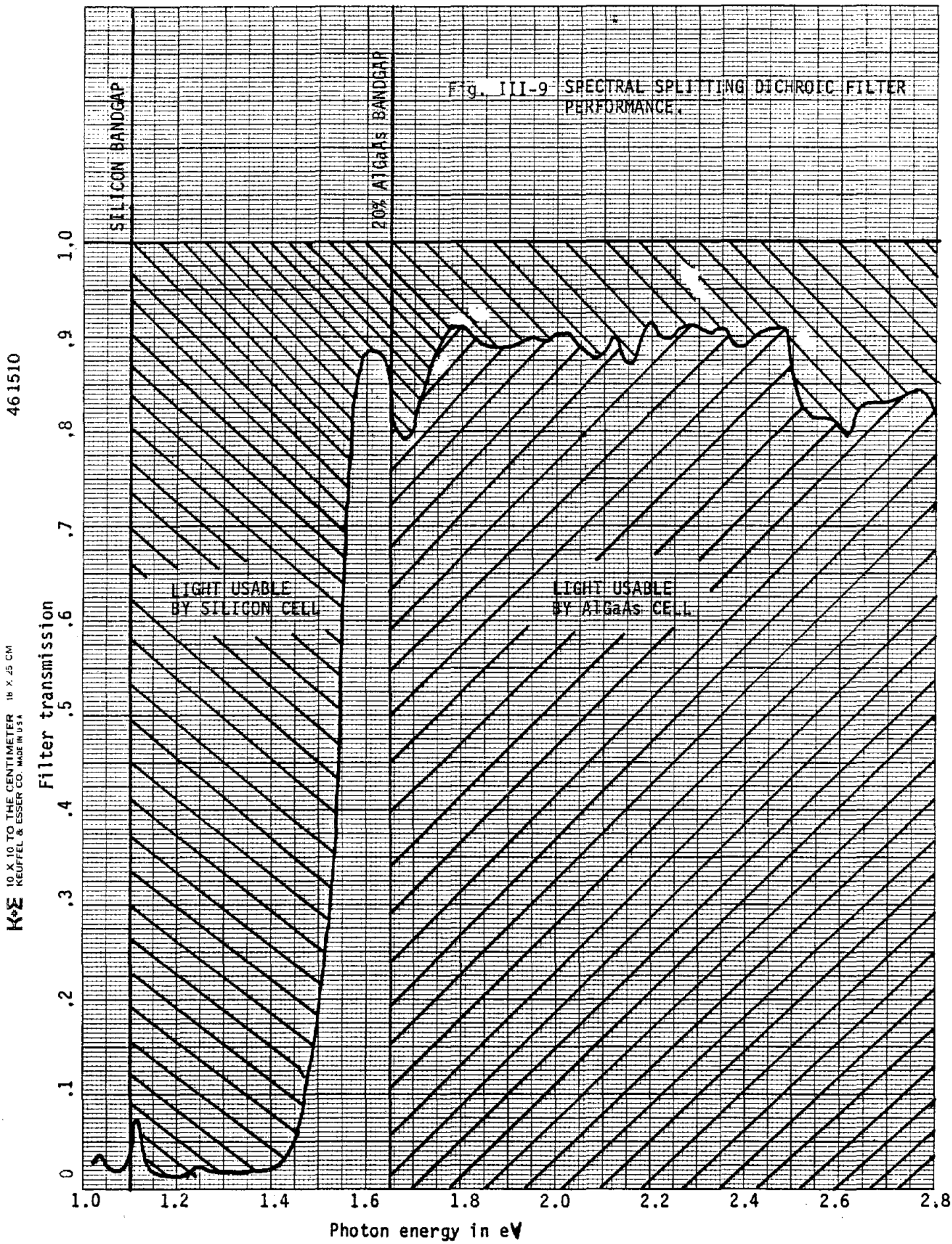

Fig. III-9 SPECTRAL SPLITTING DICHROIC FILTER PERFORMANCE.

IV. CELLS

The spectral splitter module employs ten silicon and ten $Al_{.2}Ga_{.8}As$ solar cells. These are packaged in a ceramic baseplate package developed at Varian under earlier AlGaAs/GaAs concentrator cell programs. The processes for fabricating these cells were developed under Sandia contract 07-6953.[2] The following sections describe the efforts to fabricate and test the necessary number of both silicon and AlGaAs cells.

A. The Silicon Cells

The structure of the silicon cells is shown in Fig. IV-1. With the exception of a deep emitter to enhance red response, it is a typical planar back-surface-field silicon solar cell. An n-type float zone refined Czochralski substrate, 8-mils thick, is used for starting material. The substrate is high resistivity to maintain a high lifetime. The emitter is a boron-doped layer, .7 microns thick. This provides good red response while reducing emitter resistance. The base has a diffused phosphorous layer, 1.6 microns deep, to serve as a back surface field. The front surface is not textured, but has a Si_3N_4 antireflection coating. The contacts are e-beam-deposited Ti-Pd-Ag on both front and back. The measured diffusion length of the final structure is 480 microns, or more than twice the base thickness.

Figure IV-2 shows a quantum yield measurement on such a structure. While the blue response is poor, the response in the region of 1.2-1.65 eV is quite flat, so that these cells can be expected to respond properly for the present application.

To speed up the program, it was decided to use Varian's jet impingement cooler, designed under phase one of the PRDA program.[3] This cooler accepts cells assembled into Varian's standard ceramic baseplate package.[4]

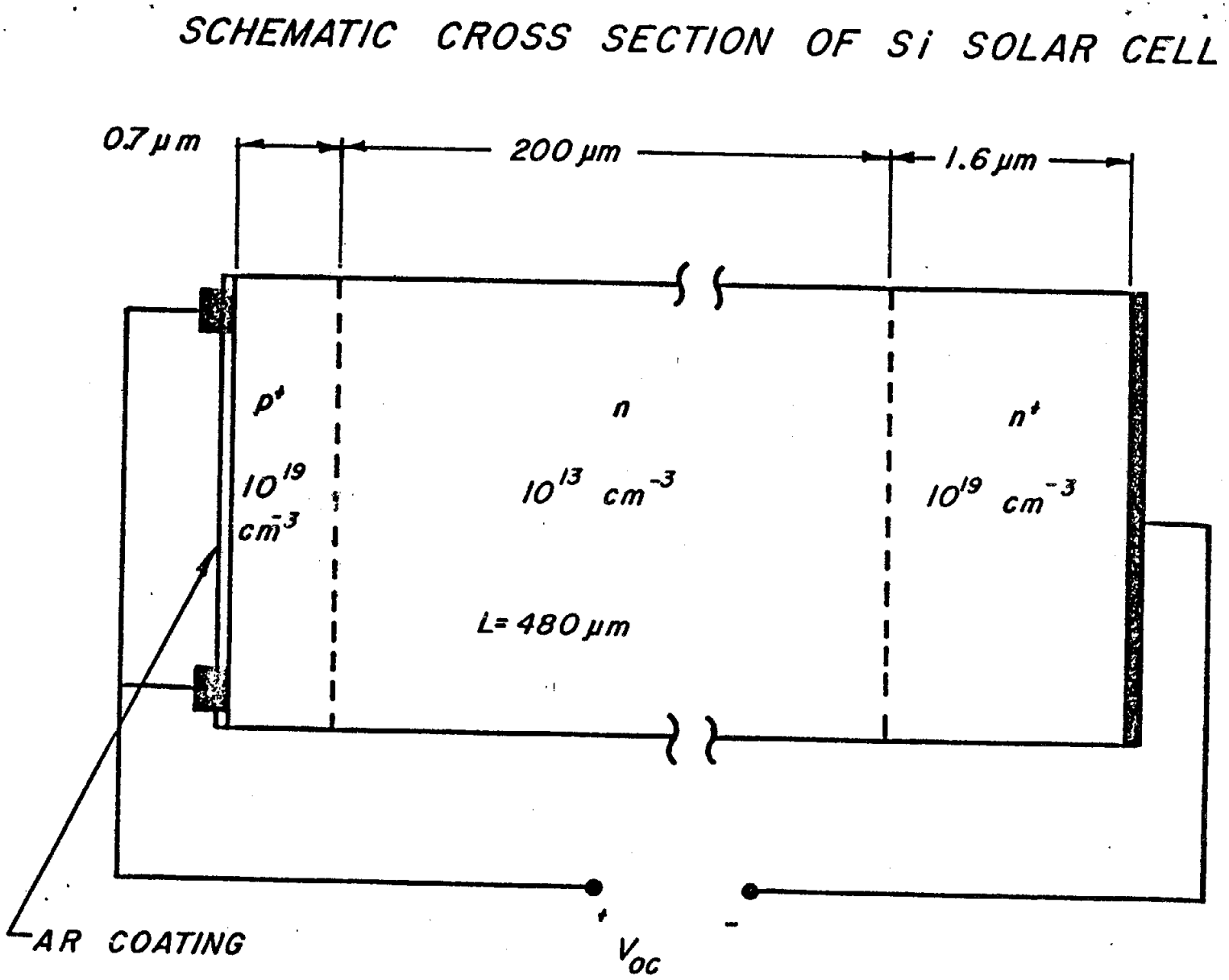

Fig. IV-1 Si Cell Structure

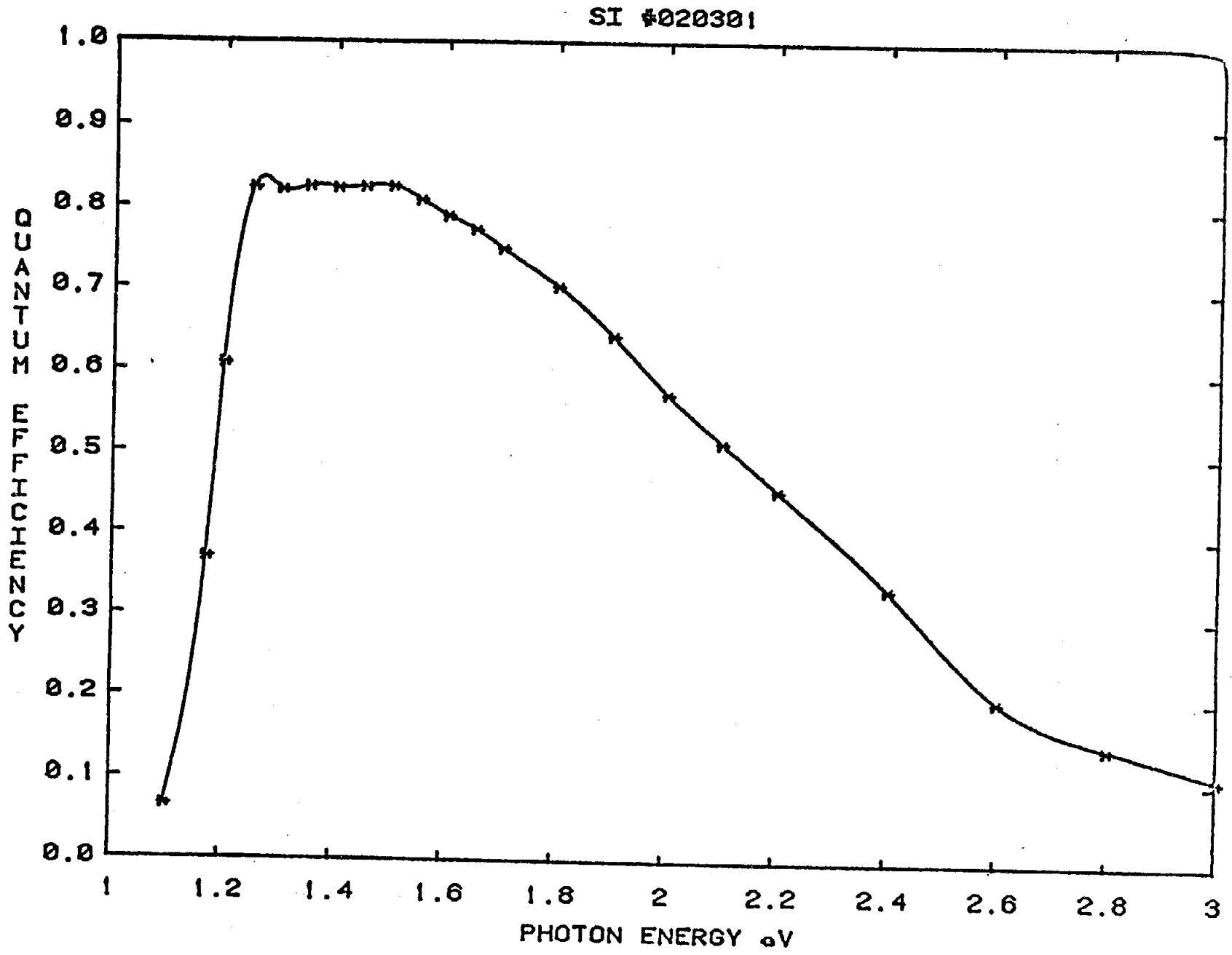

Fig. IV-2 Si Cell Quantum Yield Measurement.

This package, in turn, accepts cell die with a .5 x .5-inch format. To accommodate this format, the contact grid mask used was a radial pattern optimized for AlGaAs/GaAs cells operating at 400 suns, with a mean grid line spacing of 60 microns and an obscuration of about 11%. Since this pattern has an active area diameter of .49", a second photolithography exposure was used to reduce the diameter to .333", as shown in Fig. IV-3. As discussed in Section V-E.1, this reduction in size turns out to be unnecessary, and in fact reduces efficiency by eliminating a guard band that would have both aided in alignment and caught light spilling out of the central 1/3" area.

After packaging and flash testing, these cells were fitted with cover glasses to protect the contact grid and allow for cleaning. The cover glasses consisted of AR-coated glass discs, 1-mil thick, bonded to the front of the cells.

The characteristics of the 19 silicon cells fabricated for this program are tabulated in Table IV.1. These were obtained by flash testing. The illumination level was set at 374 suns by use of a GaAs calibration cell. These data show good uniformity in short circuit currents and open circuit voltages. It is believed that the efficiency numbers are too high, and should probably lie in the 15-16% range. The reasons for the discrepancy are not certain; however, it is postulated that the xenon flash lamp spectrum has spikes between the bandgaps of Si and GaAs. Also, the short flash rise time is not far from the lifetime in the base region of these cells. The cells marked with an asterisk in Table 4.1 were assembled into the module. It should be noted that the cells received their cover glasses <u>after</u> flash testing. This was done because the cover glass acts as a waveguide, giving an erroneous measure of short circuit current.

Fig. IV-3 Two stage masking to achieve .333" pattern on .5" die.

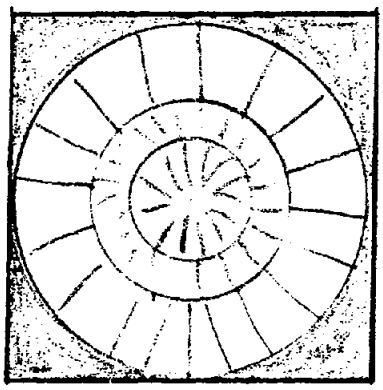

.49" grid mask pattern (detail of radial grid not shown)

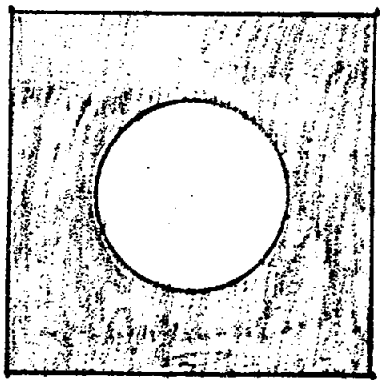

Overlay used to reduce size to .333".

TABLE IV.1 SILICON CELL FLASH TEST CHARACTERISTICS
384 Suns (GaAs calibration cell)
Packaged cells, before cover glass application.

CELL	I_{sc}	V_{oc}	FF	Efficiency
5A-9	6.83 amps	.722 volts	.61	17.3 %
*5C-7	6.81	.727	.66	19.0
5B-3	6.723	.725	.63	18.1
*5A-11	6.697	.730	.64	18.3
*5B-7	6.680	.732	.63	18.4
*5A-4	6.667	.728	.65	18.1
5B-9	6.610	.720	.55	15.6
*5B-1	6.649	.725	.63	18.1
*5A-12	6.631	.732	.68	19.5
*5C-9	6.63	.731	.71	20.0
*5B-5	6.499	.725	.67	18.8
*5A-5	6.480	.725	.71	19.2
5A-7	6.46	.727	.62	17.3
*5A-2	6.405	.723	.66	18.1
5C-10	6.310	.722	.68	17.7
5C-5	6.204	.721	.67	17.3
5C-4	6.05	.718	.69	17.1
5B-12	5.967	.712	.63	15.8
5B-6	5.986	.714	.64	16.3

Notes: The efficiencies are probably too high. See text.
The starred cells were used in the module as delivered to Sandia.

B. AlGaAs Cells

The high-bandgap AlGaAs cells are essentially identical to Varian's AlGaAs/GaAs concentrator cells,[5] except that $Al_{.2}Ga_{.8}As$ replaces the GaAs. The epitaxial structure of these devices appears in Fig. IV-4. The contact grid pattern is the same as on the silicon cell, as is the packaging. The front contact metal is a Au-Mg-Au sandwich, followed by a TiW barrier and a plated layer of Ag. In the back contact, Sn replaces the Mg and a thick deposited layer of Ag covers the TiW.

Table IV.2 lists the flash test characteristics of the 18 cells in the production run. The concentration was 393 suns and, as with the silicon cells, the cover glass was not affixed to the cell until after flash testing. It is significant to note that the characteristics of these cells are considerably more variable than seen with the silicon cells. This is in large part due to the variation in bandgap.

The cause of this variation is understood with the aid of Fig. IV-5. This shows the fraction of aluminum in the epitaxial layer as a function of the aluminum atomic fraction in the LPE melt for various growth temperatures. Note that less than .17% aluminum is required in the melt to achieve 20% AlGaAs. For a 10-gram melt, this is only 17 milligrams. To make matters worse, the slope of the curve is so steep that the growth of even a single cell depletes the melt sufficiently to significantly change the bandgap of the next cell grown with the same melt. This problem is addressed in more detail in the final report of Sandia contract 6953A;[6] as a result, it has proven difficult to consistently obtain a 1.65-eV bandgap in the AlGaAs cells over a large production run using LPE.

Figure IV-6 plots the flash test efficiency and open circuit voltages of the high-bandgap cells as a function of the bandgap of each cell. As expected, the efficiency drops slowly with increasing bandgap,

SCHEMATIC CROSS-SECTION OF 1.65 eV SOLAR CELL

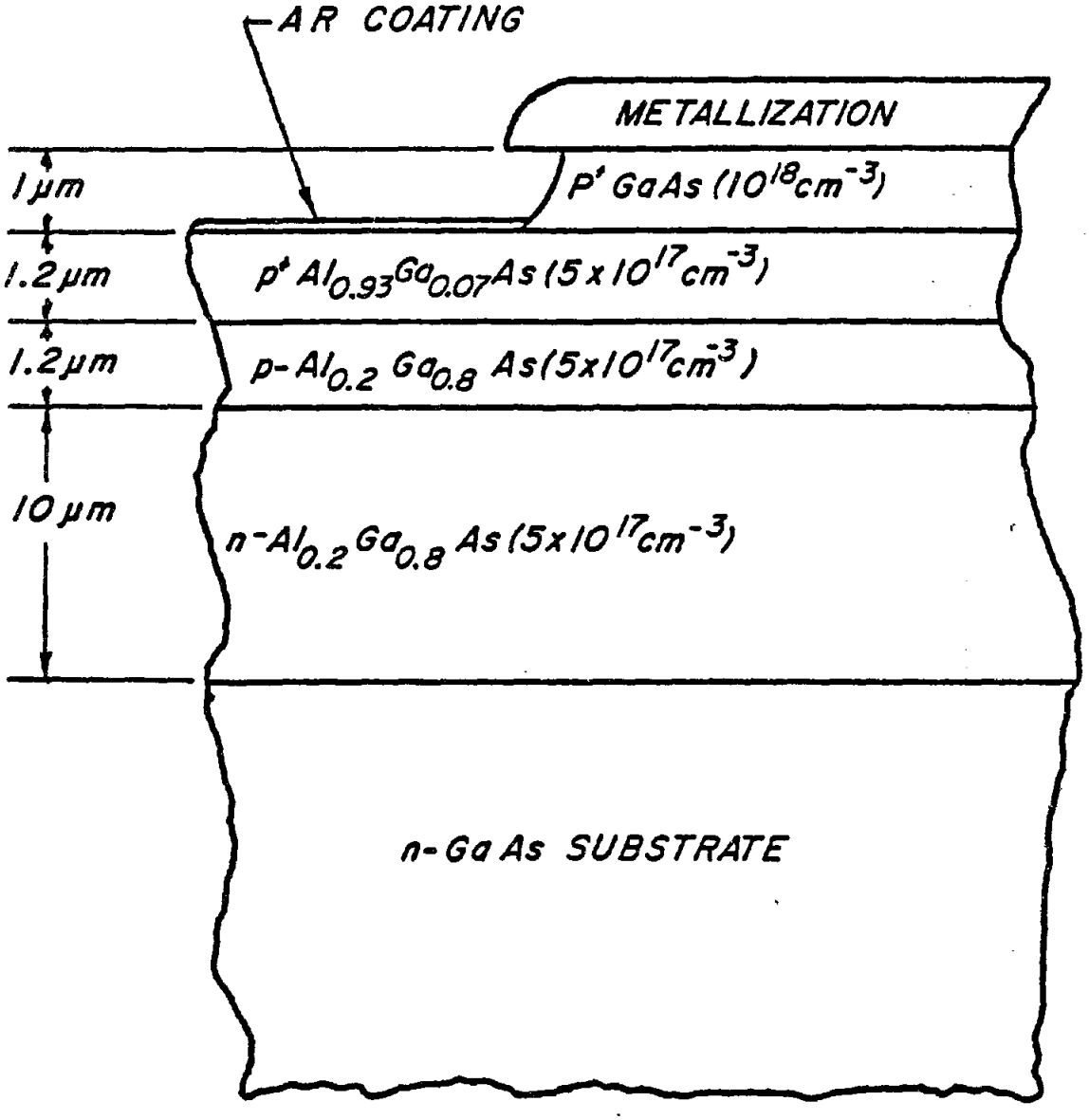

Fig. IV.4 Schematic cross-section of 1.65-eV Solar Cell. Dopings are in units of (cm^{-3}); dimensions are in microns.

TABLE IV-2 HIGH BANDGAP CELL FLASH TEST CHARACTERISTICS
393 suns (GaAs calibration cell)
Packaged cells, before cover glass application

CELL	I_{sc}	V_{oc}	ff	Efficiency	Bandgap
*3/19 ARF#1	2.961 A	1.277 V	.82	18.0 %	1.57 eV
3/18 ALR#1	2.926	1.260	.82	17.6	1.60
*3/13 CLR#1	2.894	1.303	.81	17.8	1.64
*3/20 ALR#1	2.876	1.261	.89	18.9	1.55
*3/17 ALR#1	2.856	1.292	.83	17.7	1.62
3/13 BRF#1	2.848	1.305	.81	17.3	1.65
*3/14 ALR#1	2.806	1.289	.79	16.6	1.63
*3/19 BLR#1	2.762	1.257	.81	16.3	1.56
*3/13 ALR#1	2.719	1.325	.83	17.3	1.66
*3/28 ALR#1	2.706	1.308	.84	17.3	1.64
3/25 BLR#1	2.593	1.346	.89	18.0	1.69
*3/11 BLR#1	2.571	1.351	.835	16.8	1.68
*3/27 BLR#1	2.547	1.324	.82	16.1	1.65
3/12 BLR#1	2.510	1.328	.82	15.9	1.67
3/27 ALR#1	2.485	1.311	.80	15.1	1.66
2/20 ILR#1	2.438	1.312	.76	14.1	1.66
3/26 ALR#1	2.438	1.334	.82	15.5	1.68
2/21 ILR#1	2.202	1.318	.76	12.8	1.64

Note: Cells marked with an asterisk were assembled into the module delivered to Sandia.

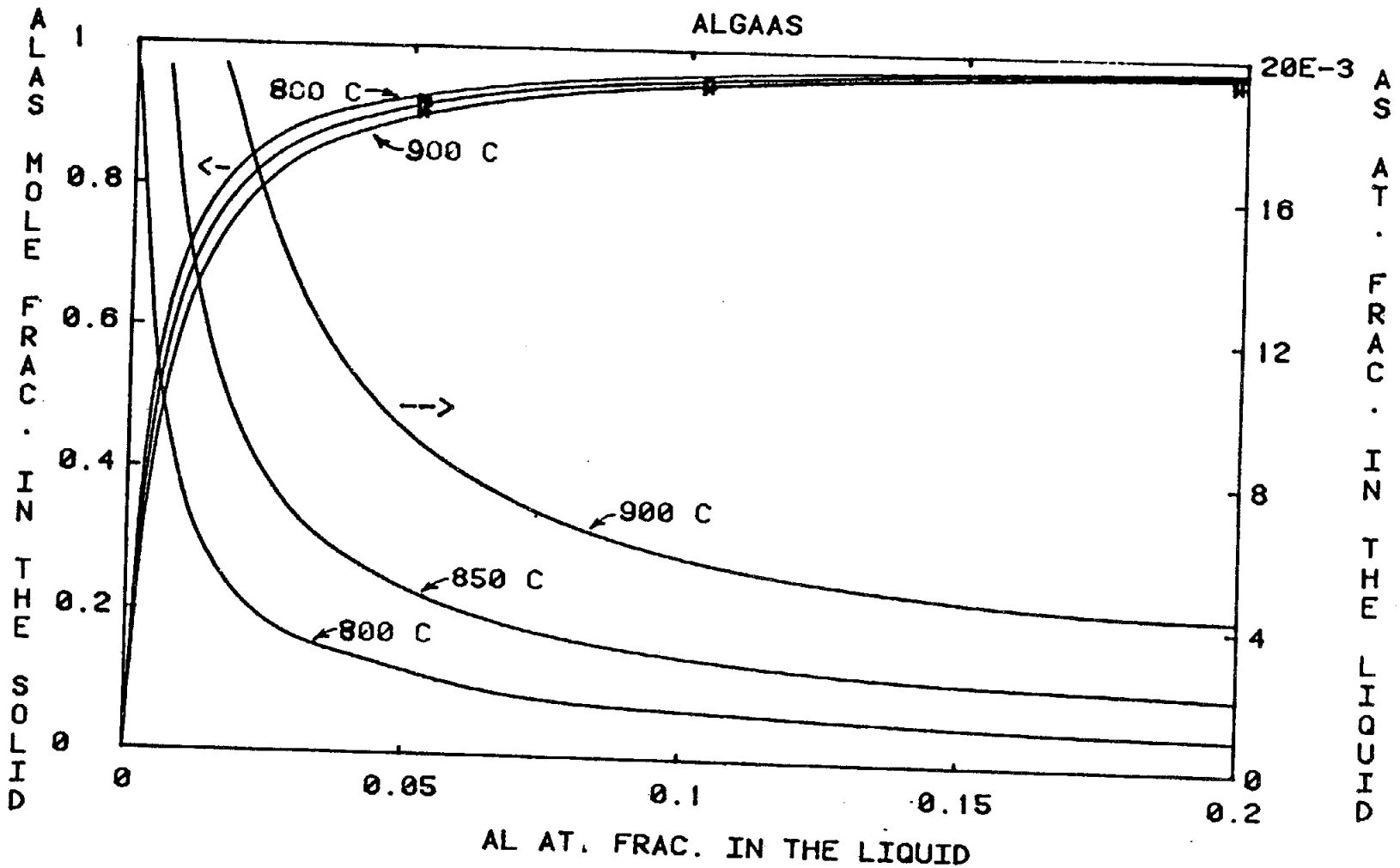

Fig. IV.5 Mole fraction of AlAs in $Al_xGa_{1-x}As$ and atomic fraction of As in solution vs. Al concentration in solution.

* Experimental points
\- Calculated from a regular solution model.

Fig. IV-6 Bandgap vs. V_{oc} and full spectrum efficiency for the $Al_{.2}Ga_{.8}As$ cells.

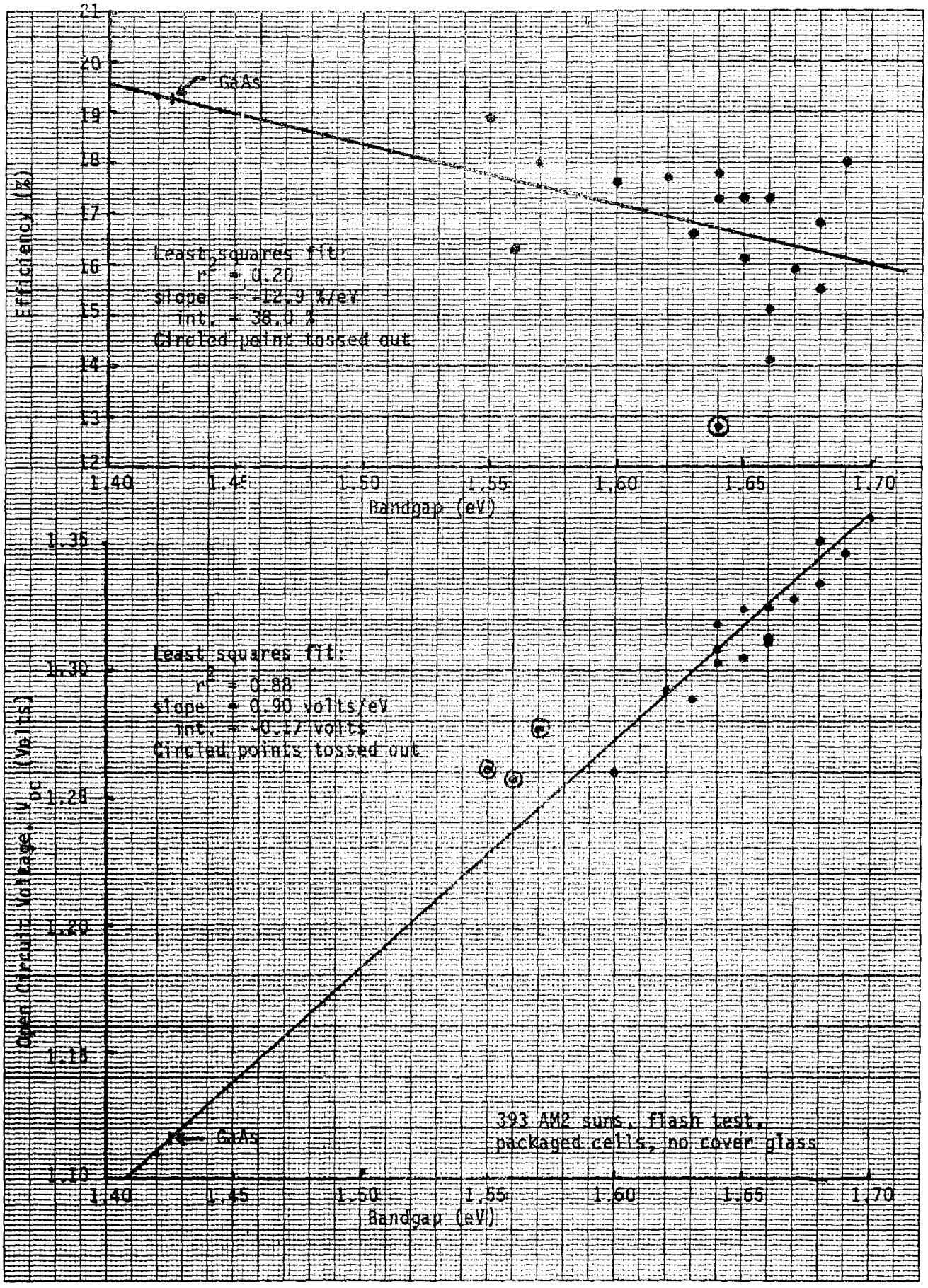

461510
K+E 10 X 10 TO THE CENTIMETER 18 X 25 CM
KEUFFEL & ESSER CO. MADE IN U.S.A.

since the cell can use less incident light for carrier generation. Except for the three lowest bandgap cells, the open circuit voltage versus bandgap values lie on a line with a slope of about unity (actually, .9). Extending the least-squares fit to the GaAs bandgap, 1.425 eV, gives an open circuit voltage of 1.12 volts, about that seen for LPE GaAs cells.

This variation has, in fact, worked to our advantage. This is because of the low cutoff of the dichroic filters. To capture some of the light above 1.55 eV sent to the high-bandgap cells, the AlGaAs cells with the lower bandgaps have been used in the module. This matter will be discussed in more detail in Sec. V-D.2.

V. MODULE TESTING

Module testing occurred during July-October, 1980, on the Varian solar-tracking array mounted on the roof of building 7 of Varian Associates in Palo Alto, California. The module was aligned and I-V characteristics of individual cells within the module were measured. A wiring configuration for the module was chosen, with cell placement based on the individual cell characteristics. The chosen configuration wired the high-bandgap (HBG) cells and the Si cells into a single output with a voltage and current at peak power point of around 5.3-5.5 volts and 8-9 amps, respectively. Finally, the I-V characteristics of the complete module were measured. The best result was 20.5% at 783 W/m^2 insolation. The module efficiency of over 20% is the highest so far achieved for a photovoltaic module.

A. Cell Alignment

Proper cell alignment is, of course, necessary for the module to achieve its peak performance. The mechanical complexity of the module makes the alignment process rather time consuming. A preliminary alignment was attempted before mounting the module on the array, by use of a laser, but that method was not found to be accurate enough. Therefore, all alignment was done with the module on the array tracking the sun. The long focal length lenses make the module quite sensitive to tracking errors. It is especially important that the tracking error not vary during alignment. A sight consisting of a small long focal length glass lens and a target upon which an image of the sun was projected was installed on the array in order to monitor the array tracking accuracy. The sight proved to be very useful in cell alignment and subsequent module testing.

The first step in module alignment is alignment of the 10 individual hexagonal cone assemblies. Each cone is aligned by placing shims between

the cone and the support frame. The cones are aligned so that light can be passed through the heat shield and fall on the HBG cell without hitting any obstruction.

The individual cells are aligned next by loosening the nuts or screws holding the cell holders to the cone; and, while monitoring the cell short circuit current, moving the cell holder laterally to achieve a peak value of short circuit current. It is also helpful to note the position of the light spot with respect to the cell surface during this adjustment (best done while wearing welding goggles). Aligning of the Si cells may also require adjustment of the angle of the spectral-splitting filter by loosening its four support screws and adjusting it for best visual alignment of light onto the Si cell.

B. Method of Testing

The test setup is shown in Fig. V-1, for tests of both the complete module and of individual cells within the module. The module was installed on the Varian two-axis solar tracking array on the roof in Palo Alto. The module was tested by measuring its I-V characteristics under computer control to find the peak power point.

The module was connected to an active load consisting of four germanium power transistors in parallel. The load is controlled by an HP-9835 computer via a programmable power supply. The 9835 computer also controls a digital multimeter which is switched through relays to read module voltage and current, and the output of an Epply normal incidence pyrheliometer (Model NIP) that is mounted on the array.

The computer program to measure the module I-V characteristics first measures the open circuit voltage and short circuit current, and then searches for the peak power point through a series of iterations in

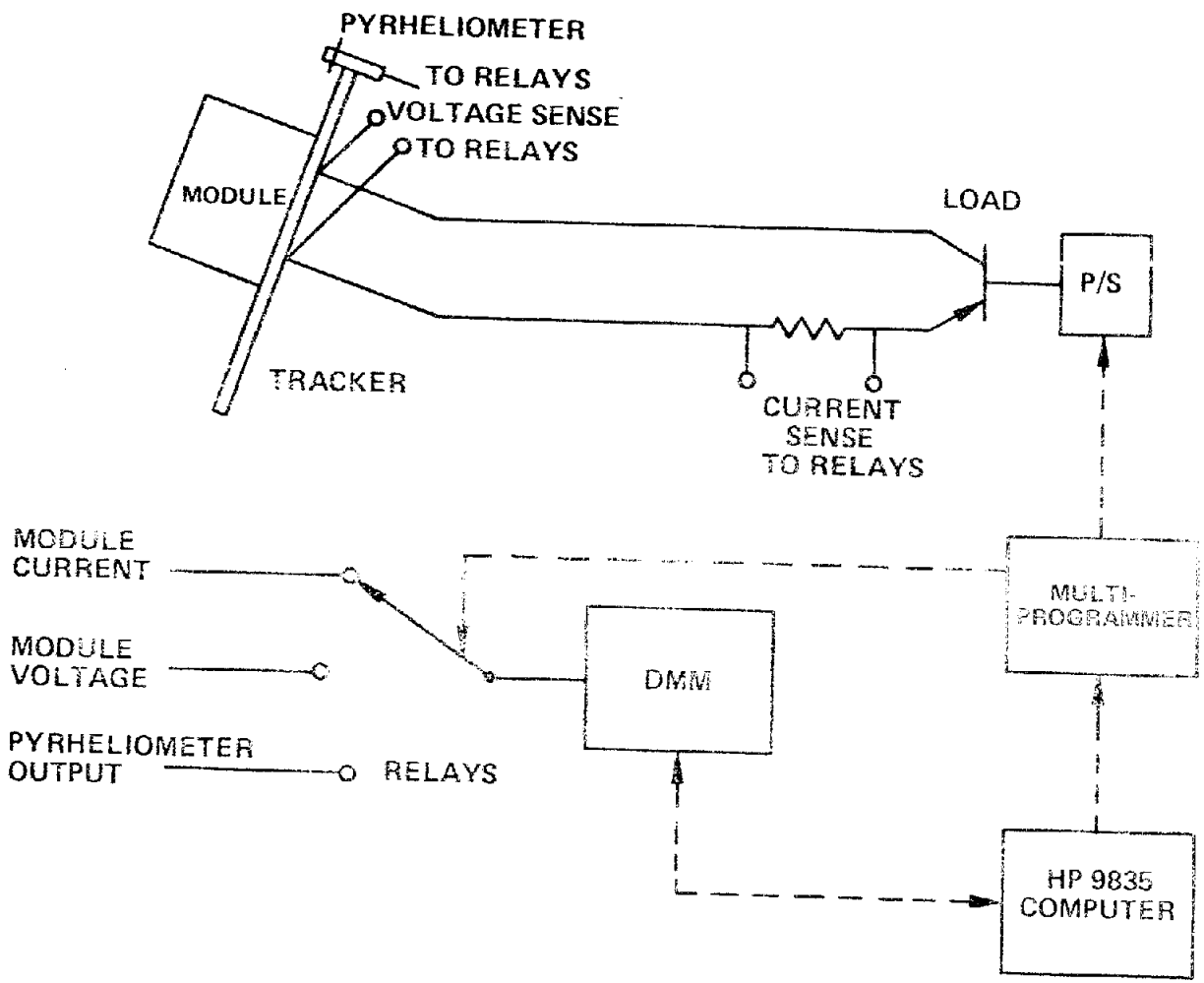

Fig. V-1 Test Setup.

which the load is set, and voltage and current are measured. Figure V-2 shows a sample of the output from the program.

The first single-cell measurements that were made on the module were done with a similar test setup, but having a different active load. Instead of the germanium power transistors, the active load consisted of a computer-controlled power supply in series with a ballast resistor and with the cell under test. That test setup was abandoned because it could not accommodate the high currents generated by the AlGaAs/GaAs cell module built under Sandia contract 42-7248, which was under test concurrently with the spectral-splitter module.

The module was cooled by a mixture of 15% ethelene glycol, 85% water. The coolant flowed through two parallel paths, one path through the HBG cells in series and one through the Si cells in series. For most of the test runs, the coolant was cooled by a chilled water loop from the building recirculating water system. The coolant temperature was not otherwise controlled. The coolant temperature was monitored by four thermistors, one each in the inlet and outlet of the Si and HBG coolant paths. The thermistors were monitored periodically, and the temperature for a particular I-V measurement was interpolated from the thermistor data.

C. Single-Cell Test Results

Cells were initially selected for the module on the basis of flash test efficiencies. With the module complete and on the array, I-V characteristics for individual cells were measured in sunlight. On the basis of these tests, three HBG cells which did not perform as well as would have been expected from the flash test data were replaced. Table V-1 lists the cells that were replaced.

```
COMPUTER CONTROLLED ROOF TEST OF CELL0
DATE:9 16/80
TIME:

DATA STORED ON FILE  RECORD 0

                V        I        P        R
     1.       6.375     .42      2.7       0
     2.        .121    0.60      1.0      750

PYRO READING: 6.282     INSOLATION830.7

                V        I        P        R
     3.       6.066    5.31     32.2      11
     4.       6.284    2.37     14.9       4
     5.        .379    0.92      3.4      26
     6.       6.280    2.37     14.9       4
     7.       5.539    8.27     45.8      19
     8.       5.879    6.86     40.3      15
     9.       1.951    8.78     17.1      23
    10.       5.735    7.62     43.7      17
    11.       3.610    8.61     31.1      21
    12.       5.639    7.90     45.0      18
    13.       4.482    8.48     38.0      20
    14.       5.631    7.99     45.0      18
    15.       5.410    8.32     45.1      19

PYRO READING: 6.287     INSOLATION839.4

ENTER SEQUENCE TO Isc
                V        I        P        R

EFFICIENCY= 20.34 Isc= 8.60 FILL FACTOR .835 Voc= 6.375 PEAK POWER= 45.785
```

```
I-V PLOT FOR CELL 0
    20.34 Efficiency
    839   Insolations
    8.60  Isc
    .835  Fill Factor
    6.375 Voc
    45.785
          Peak Power
```

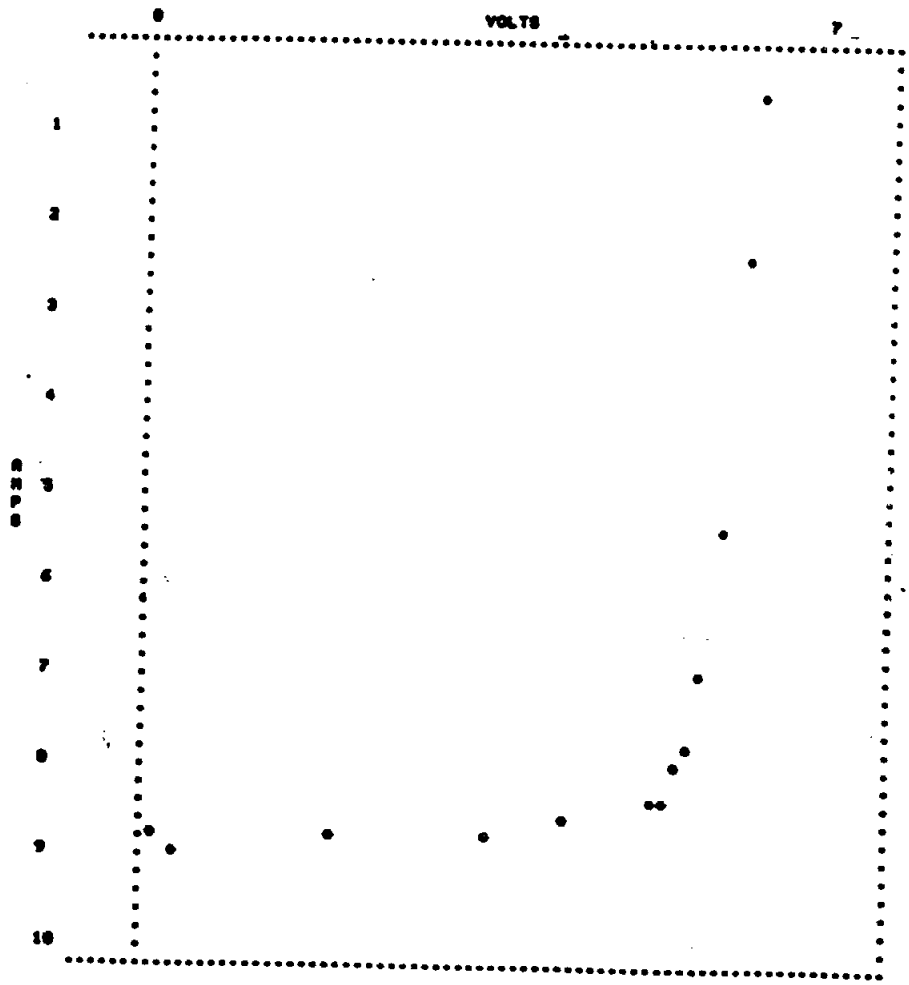

Fig. V-2 Sample output of computer and tester.

TABLE V-1

Initial Cell Replacement

Cells Removed		Cells Added	
Cell No.	Bandgap	Cell No.	Bandgap
3/18/80 ALR1	1.60	3/19/80 BLR1	1.56
3/26/80 BLR1	1.67	3/14/80 ALR1	1.63
3/25/80 BLR1	1.69	3/27/80 BLR1	1.65

The average bandgap of the cells added is 0.04 eV lower than for the cells removed. As was discussed above in Section III-B, the spectral-splitting filter cutoff was at about 1.55 eV rather than the designed cutoff of 1.65 eV. Thus the slightly lower average bandgap of the cells added helps to compensate for the filter characteristics. No filter was used in the flash testing, so the effect of the filter cutoff was not seen in that data.

Table V-2 shows roof test data for individual cells, for the cells in the module as shipped. The measured individual cell efficiencies are somewhat less than would be expected from the overall module performance, discussed below in Sec. V-E. The slightly lower cell efficiency values occur because the programmable load can only make discrete steps in resistance, and the steps are large enough that for single-cell measurements the computer is unable to find the peak power point with high accuracy. By plotting the power out versus voltage points as measured, and interpolating the peak power point, the measured peak power may be as much as 8% lower than the true peak power for the individual cell measurements.

An attempt was made to test the effect of varying the cell-to-lens spacing on cell performance. Cells were moved farther back from the lens by placing 1/8-inch spacers between the cell holders and the module

TABLE V-2

Roof Tests of Individual Cells in Module Date of 8/18/80

Cell	I_{sc} Amps	V_{oc} Volts	ff	Efficiency %	Insolation W/m^2
3/13 ALR #1	3.16	1.289	.820	15.42	807.3
3/11 BLR #1	2.94	1.312	.819	14.61	804.5
3/27 BLR #1	2.97	1.278	.827	14.43	810.8
3/28 ALR #1	3.09	1.269	.819	14.63	816.6
3/13 CLR #1	3.18	1.263	.785	14.52	810.0
3/17 ALR #1	3.22	1.247	.799	14.69	815.5
3/20 ALR #1	3.08	1.224	.833	14.18	824.3
3/19 BLR #1	3.25	1.216	.790	14.09	827.2
3/19 ARF #1	3.31	1.237	.820	15.19	823.6
3/14 ALR #1	3.15	1.248	.787	14.11	816.6
Si 5A-4	2.21	.656	.718	4.78	809.5
Si 5A-2	2.41	.661	.680	5.02	804.3
Si 5A-11	2.46	.667	.701	5.24	816.4
Si 5B-1	2.38	.663	.702	5.10	808.4
Si 5B-5	2.43	.664	.704	5.21	814.3
Si 5B-7	2.41	.666	.724	5.28	820.2
Si 5A-5	2.53	.663	.731	5.12	829.9
Si 5C-7	2.25	.660	.726	4.85	828.3
Si 5A-12	2.24	.661	.739	4.98	819.4
Si 5C-9	2.38	.667	.735	5.34	813.1

housing. Several cells were tested with varying numbers of spacers. The results were not definitive because the cell alignment was not exactly the same for the different number of spacers, since it was necessary to realign the cell for each change in number of spacers and because the insolation level changed somewhat during the time required to change the number of spacers. Nevertheless, the efficiency of the cells seemed to be slightly improved with one 1/8-inch spacer, so spacers were placed on each cell holder before the module was tested as a unit. The spacers were in place when the module was shipped to Sandia.

Measurements were also made with all the Si cells in one series string, with all the LBG cells in a series string, and with the HBG cells in two series strings of 5 cells each, each string being measured separately. Extensive measurements were not made with the cells in these configurations, but the results indicate that very little power was lost by wiring the module into the series-parallel configuration described below.

D. Wiring Configuration for the Module

The wiring configuration chosen for the module is shown in Fig. V-3. It exploits the convenient fact that at the peak power point, the Si cell voltage is very nearly half that of the HBG cell voltage. The wiring configuration consists of three parallel strings of cells, with two of the strings each consisting of 5 HBG cells in series, and the third string of all 10 Si cells in series. There is one bypass diode in parallel with each cell in the module.

The cell placement in the strings is shown in Table V-3, where the cells are listed by cell number in their arrangement within the module.

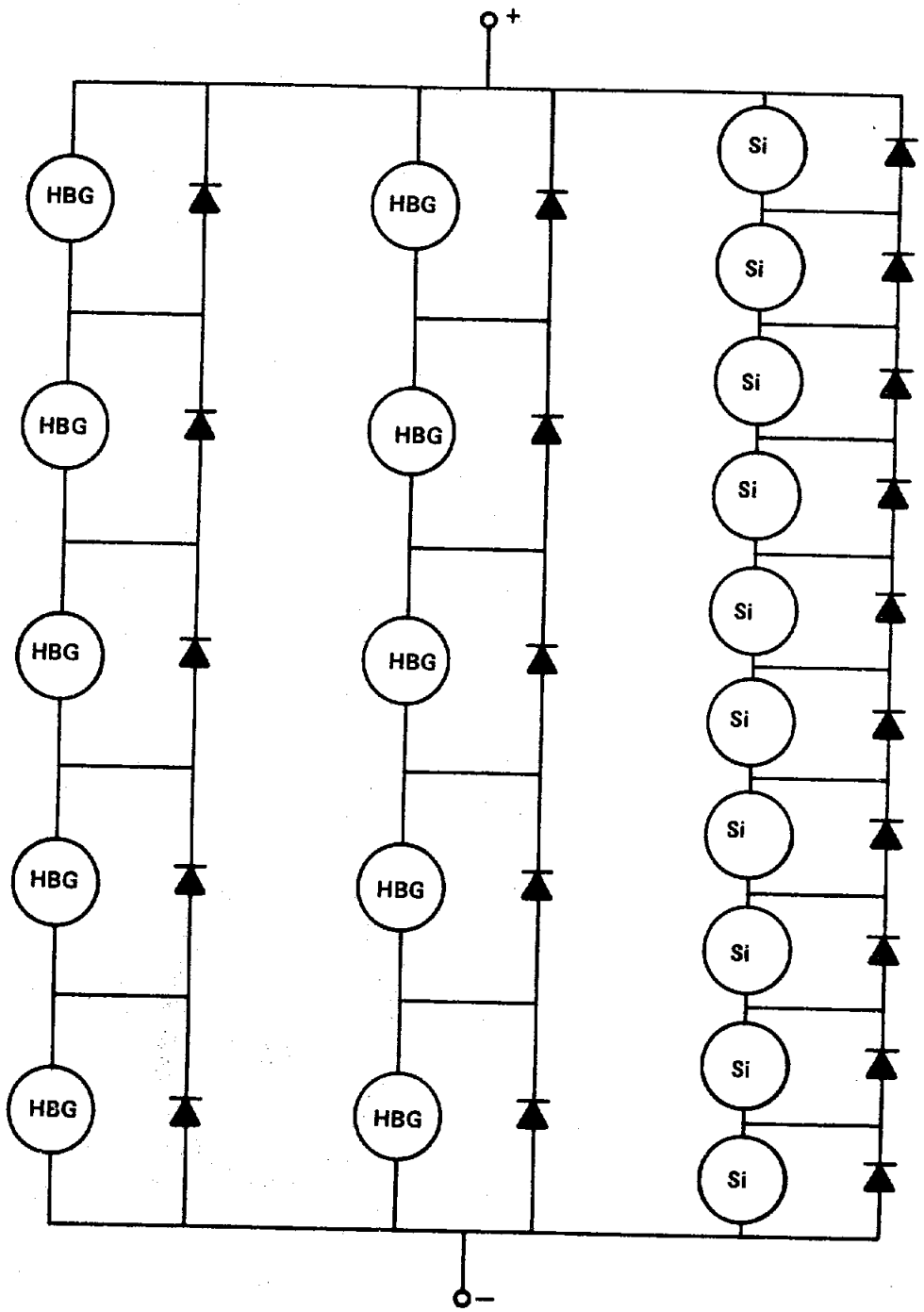

Fig. V-3 Module wiring configuration.

TABLE V-3

HBG Cell Placement in Module

HBG Cell Holder #	Series String Cell #	HBG Cell Holder #	Series String Cell #
11	3/14 ALR #1	5	3/19 ARL #1
6	3/20 ALR #1	10	3/13 CLR #1
19	3/19 BLR #1	13	3/17 ALR #1
3	3/27 BLR #1	1	3/28 ALR #1
18	3/11 BLR #1	16	3/13 ALR #1

The HBG cell placement was determined by matching the individual cell characteristics by the following criteria:

1) The current at the peak power point should be nearly the same for each cell in a series string.

2) The sum of the voltages at peak power point for each of the three series strings should be as nearly equal as possible.

The cell matching was done by hand. The module output was then simulated by a computer program which generates the module I-V curve by summing individual cell I-V characteristics. The program was used to verify that the cell placement of Table V-3 gave a higher power output than other cell placements tested.

The program was also used to simulate a different wiring configuration, one consisting of 5 cell groups in series, each group made up of two Si cells in series, and the two Si cell strings in parallel with the

two HBG cells. Using the computer program, we were not able to find a cell arrangement within that configuration that gave as high a module efficiency as the configuration of Fig. V-3, so the second configuration was not tested.

E. Module Test Results

1. Test Data

The module was wired in the configuration described in Sec. V-D and its output I-V curve was measured over a period of several days. The data from this testing is presented as Appendix A. The best results were obtained on October 8, after the lenses had been washed and the cells had been very carefully realigned. Table V-4 shows the highest efficiency data points excerpted from the data of October 8th, and Table V-5 presents all the data for October 8th. The efficiencies measured are plotted versus insolation in Fig. V-4.

TABLE V-4

Spectral Splitter -- Best Efficiencies
Data of 10/8/80

Time	Eff. (%)	Insol. (W/m^2)	Air Mass (calc)	Coolant Temp (C)	Vp (V)	Ip (A)	Pp (W)
3.57	20.53	783.4	2.10	35	5.43	7.94	43.15
3.05	20.36	847.1	1.70	36	5.52	8.38	46.25
1.37	20.21	883.2	1.43	37	5.35	8.95	47.87

The air mass listed in the tables is that calculated for the time, date, and location of the test, and does not account for actual atmospheric conditions. The insolation was measured with the normal incidence pyrhelio-

TABLE V-5

Spectral Splitter Module Test Results of October 8, 1980

Time (PDT)	Efficiency (%)	Insolation (W/m^2)	Air Mass (calculated)	Coolant Temp. (°C)	Comments
11:44	20.20	829.4	1.49	33.6	Lenses cleaned 10/7/80
11:50	20.19	840.7	1.47	33.8	
11:53	20.21	834.2	1.47	33.9	
11:55	20.18	837.7	1.46	33.9	
12:09	20.21	847.7	1.44	34.4	
12:28	20.15	853.7	1.42	35.1	
12:41	20.20	861.3	1.41	35.4	
12:52	20.21	862.8	1.41	35.7	
12:53	20.24	867.0	1.41	35.7	
1:01	20.01	862.9	1.41	36.0	
1:02	19.94	865.2	1.41	36.0	
1:14	20.16	869.2	1.41	36.3	Re-aimed array
1:15	20.19	866.6	1.41	36.3	
1:32	20.11	883.0	1.43	36.6	Coolant flow increased by removing flow meter.
1:34	20.15	876.6	1.43	36.7	
1:37	20.21	883.2	1.43	36.7	
3:02	20.28	844.7	1.69	35.6	
3:03	20.31	844.1	1.69	35.6	
3:05	20.36	847.1	1.70	35.6	
3:06	20.39	842.9	1.70	35.6	
3:08	20.38	837.4	1.72	35.6	
3:24	20.38	842.6	1.82	35.6	
3:40	20.33	812.7	1.94	35.6	
3:57	20.53	783.4	2.10	35.4	

Fig. V-4

MODULE RESULTS, OCTOBER 8, 1980

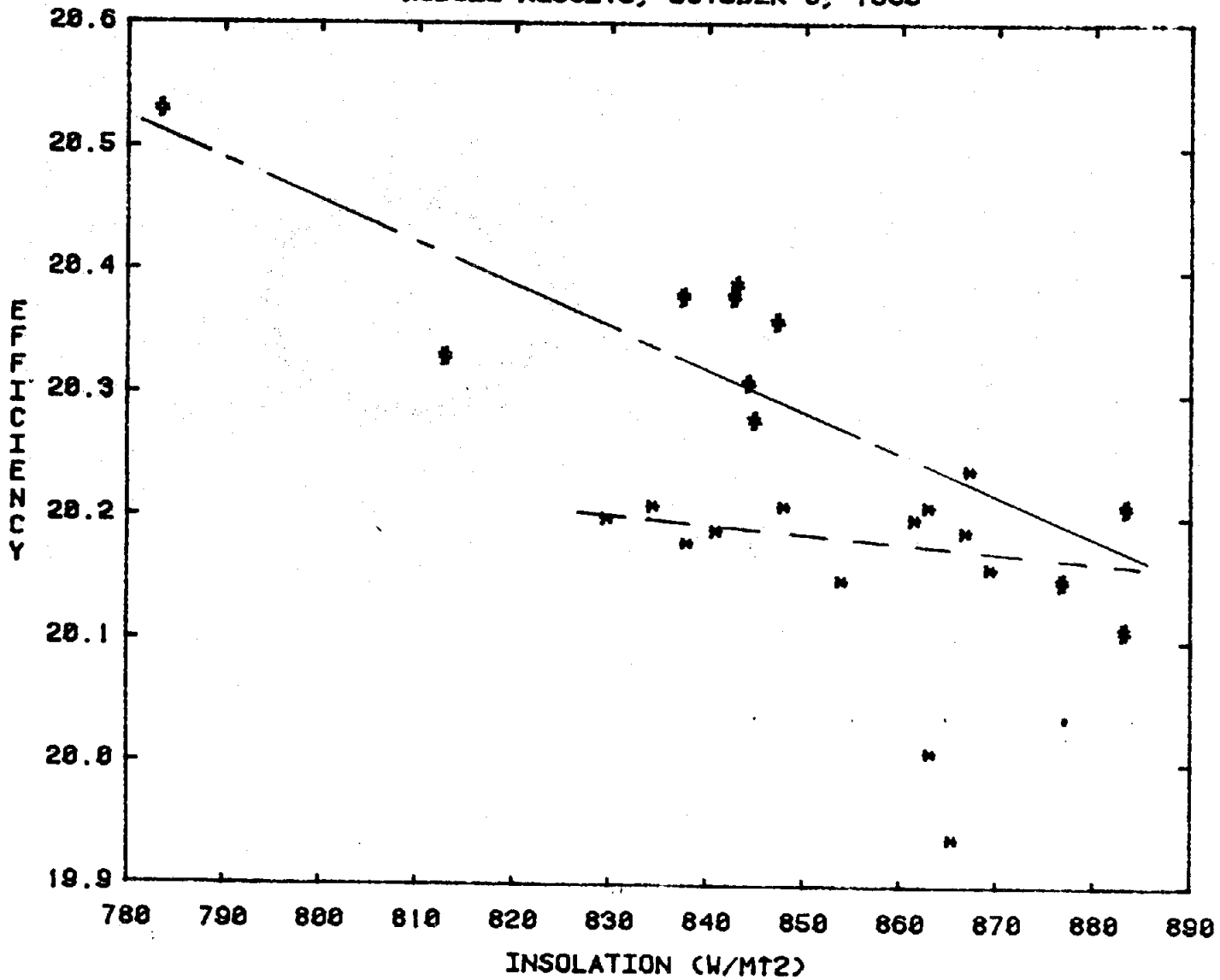

* TIME 11:44 TO 1:15
$ TIME 1:32 TO 3:57

meter for each I-V curve measured. The coolant temperature listed is the average of the measured inlet and outlet temperatures for the Si and HBG coolant paths, interpolated for the time of the I-V curve from the temperature measurements made throughout the day.

The coolant flow was about 16 gallons per hour for the whole module for all of the data measured except for some of the October 8th measurements, when the coolant flow meter was removed from the line. With the flow meter removed, the flow is estimated to be as much as twice that with the meter in place. The 16 gallons/hour flow is about twice the calculated optimum flow. No attempt was made in the measurements to find the actual optimum coolant flow, and the pressure drop across the module was not measured.

An attempt was made to do a multiple regression analysis to the measured data to fit the efficiency to an equation of the form:

$$\eta = \eta_0 + AT + BI \quad ,$$

where η is the measured efficiency, I the insolation, T the average coolant temperature, and η_0, A, and B are constants. The fit was not successful, however. The values of the constants depended on which day's data was used for the fit. Even worse, for some day's data, A or B came out positive, contrary to expectations.

Two factors which probably caused the fit to be unsuccessful are the two different types of cells in the module, and the varying atmospheric conditions during the testing. The HBG and Si cells are expected to have different temperature coefficients, and it is not obvious how the two coefficients affect the overall module performance with temperature. A further complication is the fact that the HBG and Si cells have different thermal loads.

Two atmospheric conditions which could affect the module performance are humidity and haze, both of which were present to varying degrees during the testing, but were not measured. The humidity affects the solar spectrum incident on the module, thereby affecting the module efficiency. Haze can also affect the measured efficiency by scattering the sunlight. On many of the test days, particularly in the morning, a light haze was present which, while not obscuring the sun, did scatter enough light to produce a noticeable bright area in the sky around the sun. The pyrheliometer entrance aperture is 5°43', about 10 solar diameters, so the pyrheliometer sees a larger area of sky around the sun than the module does. Thus on hazy days, the pyrheliometer reading will be higher relative to the module output than on clear days, for otherwise constant conditions.

2. Comparison to Past Split Spectrum Work

It is important to compare the results of this module work with previous split-spectrum work to suggest areas where the module can be improved.

Figure V-5 shows cell efficiency data for previous split-spectrum work at Varian performed under Sandia contract 07-6953. The results shown in Fig. V-5 are for an AlGaAs HBG cell and Si low-bandgap cell, both similar to the cells used in the module, and a spectrum-splitting filter. Note that the efficiencies in Fig. V-5 are for the combination of the cells and filter only -- lens losses (or mirror losses for the data of Fig. V-5) have been normalized out of the data. Thus the efficiency values of Fig. V-5 must be multiplied by lens losses to make a direct comparison with the module results.

The transmission of two of the 8-inch diagonal fresnel lenses on to the 1/3-inch active area of a HBG cell was measured versus lens-

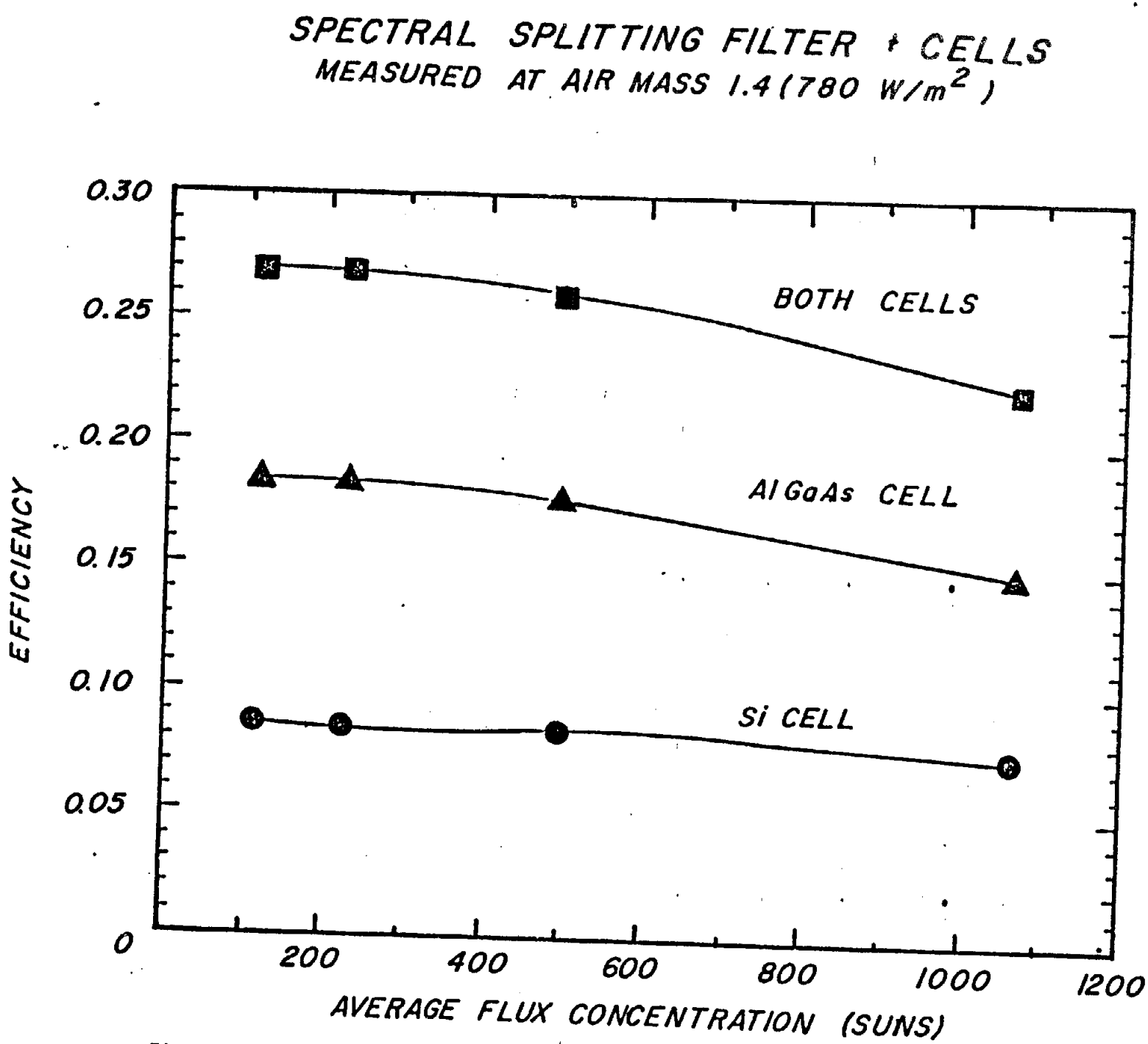

Fig. V-5. Efficiency of Cells Operating with the Spectral Splitting Filter

Fig. V-6

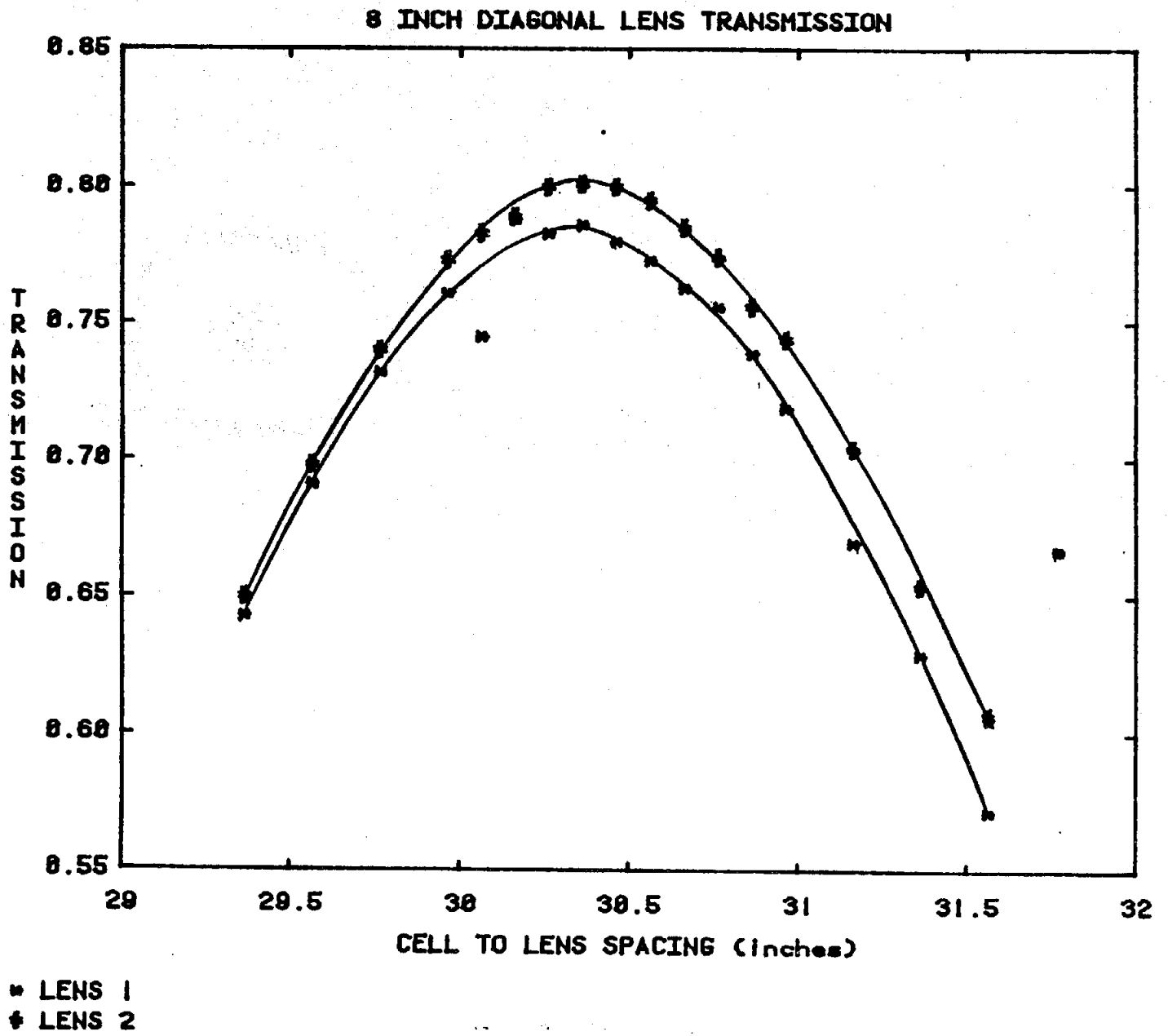
8 INCH DIAGONAL LENS TRANSMISSION
0.85
0.80
0.75
0.70
0.65
0.60
0.55
TRANSMISSION
29
29.5
30
30.5
31
31.5
32
CELL TO LENS SPACING (inches)
* LENS 1
# LENS 2

cell spacing, and is shown in Fig. V-6. The lens transmission is taken to be:

$$\text{Transmission} = \frac{\text{Measured Concentration Ratio}}{\text{Geometric Concentration Ratio}}$$

where the geometric concentration ratio for the 8-inch lens and 1/3-inch cell is 476.3 and the measured concentration ratio is the ratio between the cell short-circuit current under concentration to the cell one-sun short-circuit current (both currents normalized to insolation). The one-sun short-circuit current is measured with a light collimator.

Figure V-7 shows the efficiency of the combination of the HBG cell and Lens #1 versus lens-to-cell spacing. Note that the peak efficiency occurs at about 30.5 inches spacing, the same spacing at which the peak in transmission falls, and also the spacing which was used for the design of the module. As Fig. V-6 shows, the peak lens transmission is between 78 and 80%. A peak transmission of 85% would have been expected from our work with fresnel lenses for the GaAs solar cell module, while the raytrace design of the lens indicates that 90% transmission should be achieved.

The lower-than-expected transmission is due to light spillover beyond the 1/3-inch active area of the cell. To assess the magnitude of this effect, one of the lenses was retested using a 1/2-inch GaAs cell as a detector. The transmission onto the 1/2-inch active area is compared to that onto the 1/3-inch cell in Fig. V-8. The peak transmission for the larger cell is 85%, clearly illustrating that a significant amount of light is lost to spillover on the 1/3-inch cell. This measurement does not indicate how far beyond the 1/3-inch area that the spillover falls, but visually it appeared to lie in a ring 1-2 mm beyond the edge of the 1/3-inch active area.

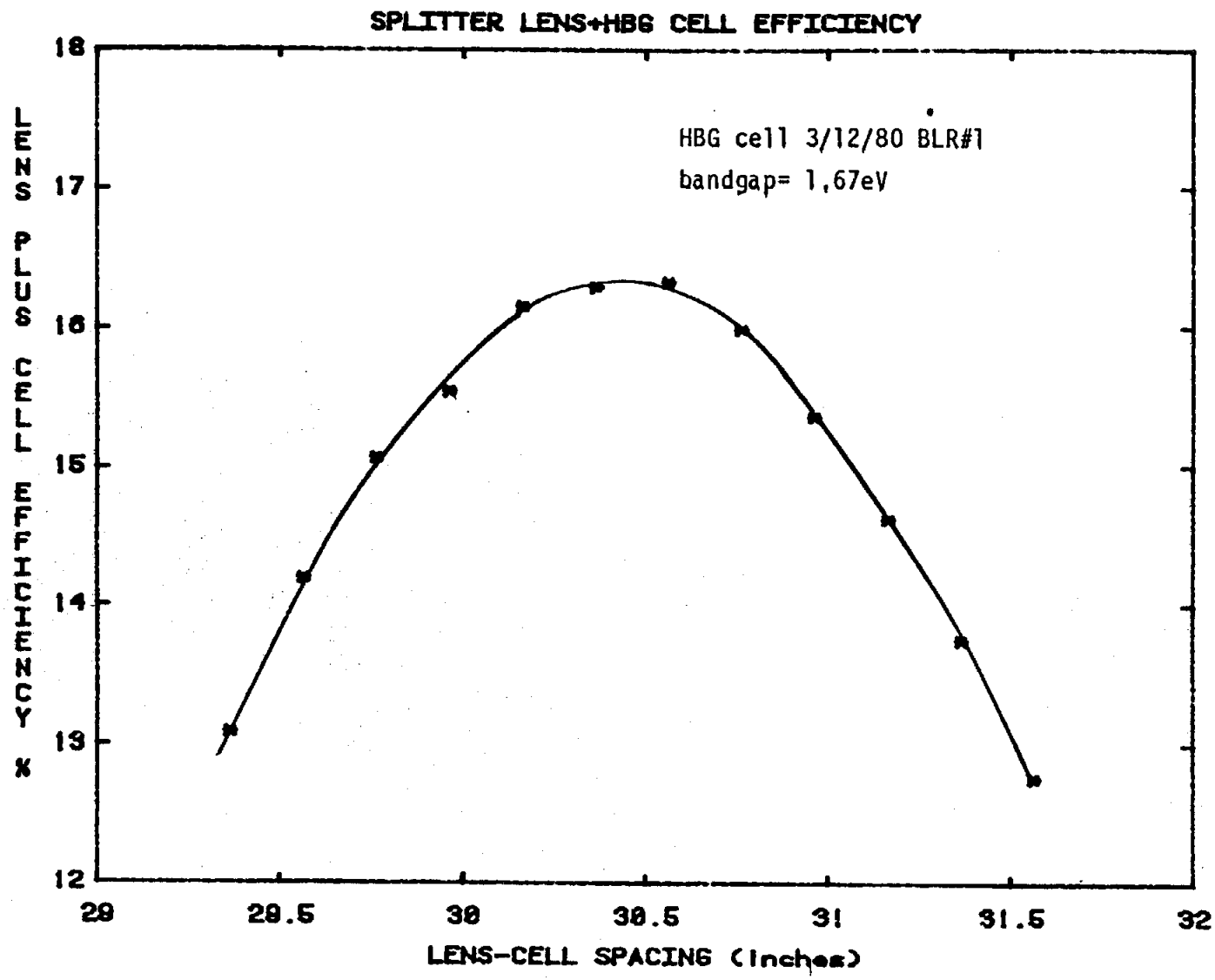
SPLITTER LENS+HBG CELL EFFICIENCY
HBG cell 3/12/80 BLR#1
bandgap= 1.67eV
LENS PLUS CELL EFFICIENCY %
18
17
16
15
14
13
12
29
29.5
30
30.5
31
31.5
32
LENS-CELL SPACING (inches)

Fig. V-7

Fig. V-8

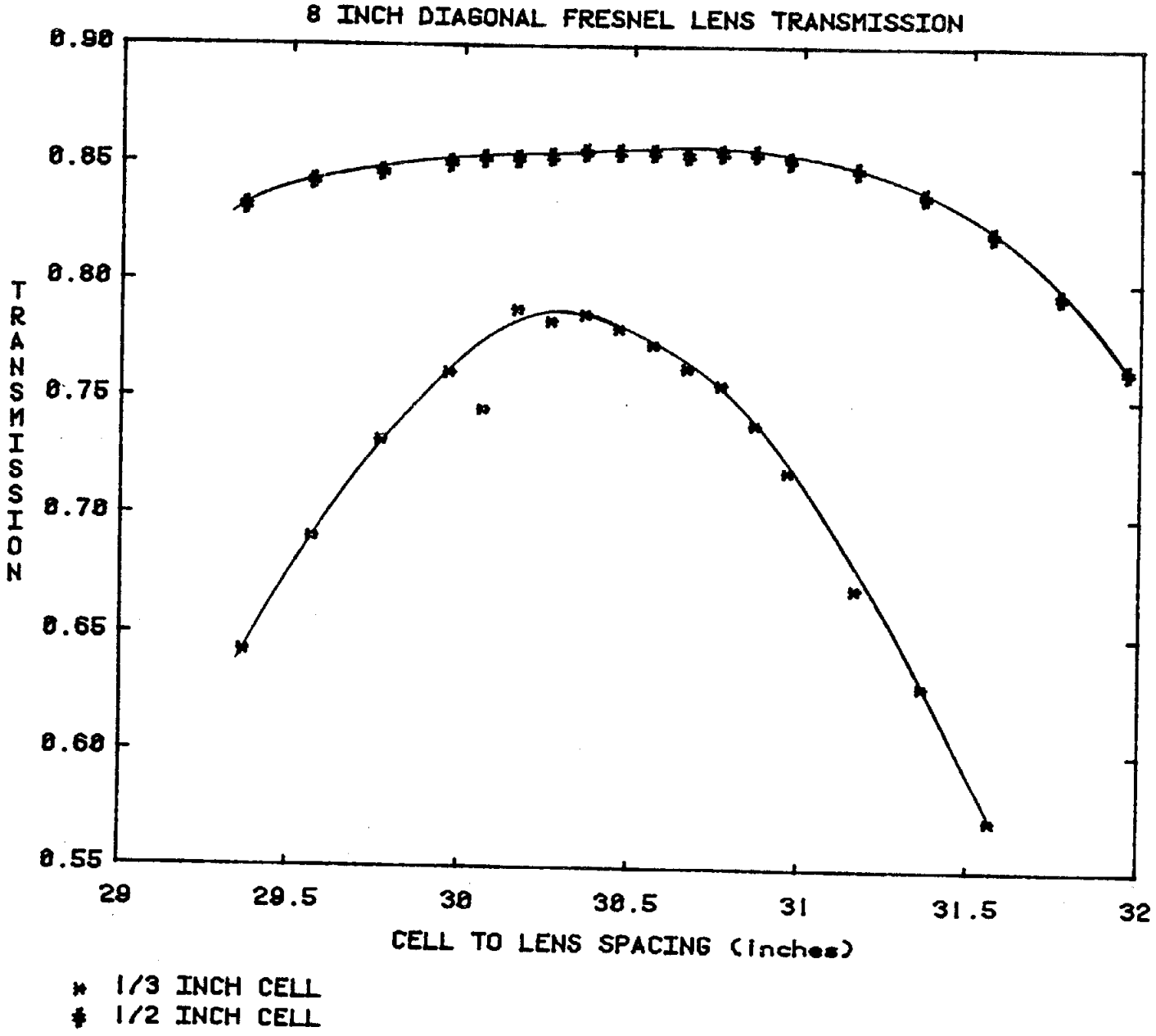
8 INCH DIAGONAL FRESNEL LENS TRANSMISSION
TRANSMISSION
0.90
0.85
0.80
0.75
0.70
0.65
0.60
0.55
29
29.5
30
30.5
31
31.5
32
CELL TO LENS SPACING (inches)
* 1/3 INCH CELL
* 1/2 INCH CELL

Taking the higher of the two lens transmission measurements onto a 1/3-inch cell of 80% peak and normalizing the peak module efficiency of 20.5% to a lens transmission of 100%, as was done for the data of Fig. V-5, the efficiency is 25.6%. A lens transmission of 80% corresponds to a concentration of 382.5. The data of Fig. V-5 was measured at the same insolation level for which the 20.5% module efficiency was measured. At 382 suns, the efficiency for both cells together of Fig. V-5 was 26.5%. Thus the lens transmission accounts for almost all of the difference between the present module results and the previous cell results.

Another difference between the previous results and the module results is that a different spectral-splitting filter was used. Figure III-6 of the final report on Sandia contract 07-6953 shows the filter transmission for the filter used for the previous work. The peak transmission for that filter was 97%, compared to about 91% for the filters used in the module. Thus more light was transmitted to the HBG cell with the older filter. Since the HBG cell efficiency is greater than the Si cell (which receives the light not transmitted to the HBG cell), the old filter would have given a somewhat higher efficiency for the two cell plus filter combination.

The old filter had about the same 1.55-eV cutoff as the filters used in the module. If the cutoff had been at 1.65 eV, the design bandgap for the HBG cell, the efficiency would have been higher for both the previous results and for the module. The light between 1.55 eV and 1.65 eV incident on the HBG cell is wasted. A calculation was made of the added efficiency to be obtained by directing the light between 1.55 eV and 1.65 eV onto the Si cell. The calculation assumes the same filter characteristics as was used in the module, but rigidly shifted upward by .1 eV. The calculation integrates the product of the filter characteristic, a typical Si cell quantum yield curve, and the solar spectrum. The calculation shows that the Si cell short-circuit current

would increase by about 20% for both an AM1 and AM2 solar spectrum with the filter cutoff at 1.65 eV. This would increase the effective Si cell efficiency to about 6% from its 5% value, and would thus raise the module efficiency by one percentage point - to 27.5%. Referring back to Fig. V-5, this is seen to be about 1% point higher than the results reported earlier with a single converter.

VI. CONCLUSION

This module represents the first demonstration of the concept of spectrum splitting at a level beyond single cells. While the component count is high and the filters quite costly, the module has a very important advantage in that all the parts -- cells, filters, lenses -- are readily accessible. By looking at the performance of these components individually and together as a system, it is possible to learn how much performance can be gained by moving to the spectrum-splitting approach to concentrator photovoltaics.

The best reported module performance at the time of this writing was achieved with the Varian GaAs concentrator cell module, manufactured under Sandia contract 42-7248. Under conditions similar to those which the spectrum splitter was tested, that module demonstrated about 17% conversion efficiency. The best silicon cell module of comparable size achieves about 12% conversion efficiency. Thus, the best measured efficiency of 20.5% represents an improvement of about 20% over the GaAs module and about 70% over the silicon module.

A number of loss mechanisms have been identified. These include the following:

- The filters cut off .1 eV too low.

- The cell active area is too small; going to a .5-inch diameter active area would collect a significant amount of spillover. This would also provide a guard band to simplify alignment.

- The cells were grown with Liquid Phase Epitaxy (LPE). Current results with Organometallic Vapor Phase Epitaxy (OM-VPE) indicate that the average efficiency of the high-bandgap cells would be improved with this technique.

A balance sheet of the collective effect of these various improvements is presented in Table VI-1.

TABLE VI-I

Effect of Losses

Measured performance	20.5%
Improved filters	1.0%
Improved cells	
Collected spillover	1.2%
Alignment (guard band)	.5%
OM-VPE AlGaAs cells	1.5%
Potential performance	24.7%

While Table VI-1 is admittedly somewhat speculative, the estimated effect of each of the loss factors is supported by the measurements performed, as described in Sec. V. Note that the 24.7% potential performance represents a filter plus cell efficiency of about 29%, assuming an 85% lens transmission to .5-inch-diameter cells. The 24.7% potential performance would represent an improvement of 45% over the GaAs module, and about 100% over the best silicon module. Thus the spectrum-splitting module represents a significant technological step forward. The only problem is to build it at reasonable cost.

The two factors contributing to excessive cost are the filter and the long focal length design, requiring greater tracker accuracy (hence higher tracker cost) and more materials. These drawbacks can be overcome by various approaches that are now being pursued. These include reflective splitters, mechanically-stacked cell configurations, and monolithic multijunction cells. These various alternatives are presently under study, supported by Sandia and SERI contracts.

APPENDIX A: SUMMARY OF TEST DATA FOR SPECTRAL SPLITTER

Date: 9/16/80

Time	Eff. (%)	Insol. (W/m^2)	Air Mass	Coolant T (°)	Comments
--	20.34	839.4	--	--	cloudy day
Date: 9/19/80					
2:13	19.96	878.1	1.32	36.0	
2:21	19.84	876.1	1.34	36.0	
2:35	19.72	879.1	1.37	36.0	
2:38	19.91	877.4	1.38	36.0	
2:39	19.84	875.2	1.38	36.0	
2:52	19.81	873.8	1.42	36.0	
2:53	20.17	872.8	1.42	36.0	
3:26	19.99	857.1	1.55	36.4	
3:30	20.14	857.1	1.57	36.4	
3:32	20.03	855.3	1.58	36.3	
3:33	20.15	852.9	1.59	36.3	
5:04	20.30	754.6	2.55	35.5	
5:10	20.22	743.4	2.68	35.1	
Date: 9/22/80					
9:16	20.38	781.4	2.31	22.4	
9:33	20.37	797.9	2.08	25.0	
9:37	20.26	802.3	2.04	25.6	
9:45	20.39	818.3	1.95	26.9	
9:46	20.29	819.1	1.94	27.0	
10:00	20.24	834.6	1.82	29.0	
10:06	20.16	844.6	1.77	29.8	
10:20	20.02	855.5	1.68	31.5	
10:29	19.93	862.3	1.62	32.3	
10:34	19.94	867.4	1.60	32.9	
10:45	19.94	876.0	1.54	33.8	
12:34	19.70	914.6	1.29	39.9	
12:56	19.53	916.2	1.28	40.7	
12:58	19.55	916.2	1.28	41.1	

Time	Eff. (%)	Insol. (W/m^2)	Air Mass	Coolant T (°)	Comments
Date: 9/22/80 (cont.)					
1:04	19.44	914.7	1.28	41.1	
1:43	19.30	907.7	1.30	42.4	
2:14	19.42	897.6	1.35	43.0	
3:00	19.49	834.6	1.48	43.6	
3:23	19.63	869.2	1.58	43.7	
3:42	19.85	855.3	1.68	36.7	coolant chiller turned on
4:02	20.06	840.6	1.83	34.4	
4:29	19.40	802.9	2.10	32.8	
4:34	19.42	802.4	2.16	32.6	
4:40	20.04	779.2	2.24	32.4	
4:42	19.90	771.7	2.27	32.3	
4:43	20.06	769.2	2.29	32.3	
Date: 9/23/80					
10:30	20.06	855.0	1.63	27.7	smog on horizon
10:37	20.08	860.3	1.59	28.3	
10:39	20.09	861.1	1.58	28.4	
10:57	19.98	875.3	1.50	29.5	wire loose on terminal
10:58	20.11	877.2	1.49	29.5	
1:20	19.87	911.5	1.29	33.9	
1:22	19.94	911.7	1.29	33.9	
1:37	19.61	911.2	1.30	34.5	
Date: 9/26/80					
4:49	20.23	689.5	2.51	--	Replaced HBG cell 3/11/80 BLR #1 with 3/13/80 BLR #1 and Si cell Si5A-2 with Si5A-9
4:58	20.46	675.0	2.69	--	
5:07	20.44	663.6	2.90	--	
5:10	20.14	654.6	2.98	26.5	

Time	Eff. (%)	Insol. (W/m^2)	Air Mass	Coolant T (°)	Comments
Date: 10/1/80					
3:00	19.92	768.0	1.58	--	Still have two replacement cells in module
3:19	19.95	771.7	1.68	--	
3:22	19.89	768.1	1.69	--	
3:43	19.97	753.1	1.83	36.7	
3:44	19.99	754.2	1.84	36.7	
3:54	19.65	754.4	1.93	36.5	
5:04	18.73	580.8	3.05	35.1	
Date: 10/2/80					
8:21	18.07	427.6	4.35	22.8	Light haze and smog. Still have 2 replacement cells in module.
8:23	18.02	432.4	4.23	23.2	
8:28	18.64	456.2	3.96	23.6	
8:31	18.51	472.1	3.82	23.7	
8:39	19.55	524.0	3.48	24.6	Adjusted tracker alignment
8:52	19.68	564.1	3.06	25.4	
8:57	19.63	584.0	2.92	26.1	
8:58	19.52	591.1	2.90	26.1	
9:50	20.05	741.8	2.05	29.4	Realigned 2 cells
9:52	20.17	743.5	2.03	29.6	
9:57	20.18	752.2	1.98	29.8	
10:12	20.08	766.9	1.85	30.5	
10:15	20.05	774.9	1.82	30.6	
10:33	20.17	792.3	1.70	31.4	
10:34	20.18	793.1	1.70	31.4	
10:37	20.15	803.7	1.68	31.6	
10:53	20.02	817.0	1.60	32.2	
10:56	20.10	817.1	1.59	32.3	
10:57	20.10	819.2	1.58	32.4	

Time	Eff. (%)	Insol. (W/m^2)	Air Mass	Coolant T (°)	Comments
Date: 10/2/80 (cont.)					
11:30	19.91	836.7	1.47	33.6	
11:31	20.10	836.2	1.46	33.6	
11:33	20.04	839.0	1.46	33.7	
11:34	19.97	837.8	1.46	33.7	
4:27	20.27	753.4	2.33	29.0	
4:43	20.31	726.7	2.60	39.2	Replaced 3/13/80 BLR#1 with 3/11/80 BLR#1.
4:45	20.28	722.3	2.64	39.2	
Date: 10/6/80					
2:06	20.12	754.2	1.46	30.4	Muggy day, overcast in morning. Still have 1 Si cell replaced.
2:09	20.04	750.5	1.47	30.5	
2:22	19.88	751.1	1.50	30.7	
2:37	19.96	746.7	1.55	31.0	
2:49	20.11	738.1	1.60	31.2	
3:18	20.21	733.4	1.75	31.3	
3:20	20.19	728.6	1.76	31.3	
3:22	20.22	730.6	1.77	31.3	
3:24	20.21	727.8	1.78	31.3	
3:27	20.16	720.2	1.80	31.3	
4:10	20.05	657.3	2.21	31.0	Replaced cell Si 5A-9 with Si 5A-2 (i.e., back to cell complement of runs dated 9/13/80 - 9/23/80
4:11	20.16	653.7	2.22	31.0	
4:17	19.96	640.5	2.30	30.9	
4:19	20.24	639.4	2.33	30.8	
4:44	19.78	580.8	2.77	30.0	
4:46	19.97	572.1	2.82	30.0	

Time	Eff. (%)	Insol. (W/m^2)	Air Mass	Coolant T (°)	Comments
Date:	10/7/80				
2:20	19.98	791.9	1.51	35.8	
2:21	19.89	785.0	1.51	35.8	
2:56	20.12	776.6	1.64	36.1	
3:16	19.96	765.4	1.75	36.2	
3:45	20.15	747.9	1.96	36.1	
3:47	20.15	744.6	1.98	36.1	
4:15	20.03	723.4	2.30	35.9	
4:16	20.15	718.6	2.31	35.9	
4:44	20.54	657.9	2.82	35.4	Washed lenses
4:45	20.58	654.6	2.84	35.4	
4:52	20.49	638.9	3.01	35.2	
4:53	20.12	634.6	3.04	35.2	

NOTE: Data for 10/8/80 is in text.

REFERENCES

1. R. L. Moon, L. W. James, H. A. Vander Plas, T. O. Yep, G. A. Antypas and Y. G. Chai, "Multigap Solar Cell Requirements and the Performance of AlGaAs and Si Cells in Concentrated Sunlight," Record 13th Photovoltaic Spec. Conf., 859 (1979).

2. L. W. James, H. A. Vander Plas and R. L. Moon, "Novel Solar Cell Concentrator Photovoltaic Converter System," Final Report Sandia Contract 07-6953 (1979).

3. J. S. Escher, "R&D on Long Wavelength Bias-Assisted Photoemitter," Final Report ARO Contract DAAG-29-78-C-0035, Phase I (to be published).

4. B. R. Cairns, "Near-Term Implementation of Production Cost Reduction for Photovoltaic Concentrator Array," Final Report Sandia Contract 13-2357 (1980).

5. R. R. Saxena, V. Aebi, C. B. Cooper III, M. J. Ludowise, H. A. Vander Plas, B. R. Cairns, T. J. Maloney, P. G. Borden and P. E. Gregory, "High-efficiency AlGaAs/GaAs Concentrator Solar Cells by Organometallic Vapor Phase Epitaxy," J. Appl. Phys. 51, 4501 (1980).

6. H. A. Vander Plas and P. E. Gregory, "Further Development of a Novel Solar Cell Concentrator Photovoltaic Converter System," Final Report Sandia Contract 07-6953A (1980).

DISTRIBUTION LIST:

Acurex Corporation (3)
Attn: George Sutton
Bob Spencer
John Kull
485 Clyde Avenue
Mountain View, CA 94042

Aerospace Corporation
Attn: Ed Simburger
2350 El Segundo Blvd.
El Segundo, CA 90266

Alliance Tool Corp.
Fresnel Optics Division
Attn: Helmut Walter
1300 Mt. Read Blvd.
Rochester, NY 14606

Applied Solar Energy Corp. (3)
Attn: Steve Olah
Frank Ho
Ken Ling
15251 E. Don Julian Road
City of Industry, CA 91746

ARCO Power Systems
Attn: Floyd Blake
Suite 307
7061 S. University Blvd.
Littleton, CO 80122

Arizona State University (2)
Attn: Charles Backus
Robert Sanderson
College of Engineering
Tempe, AZ 85281

Ray Bahm & Associates
Attn: Ray Bahm
2513 Kimberly Court NW
Albuquerque, NM 87130

Battelle
Attn: Don Carmichael
505 King Avenue
Columbus, OH 43201

The BDM Corporation (3)
Attn: Tim Lambarski
Wayne Kauffman
Bill Schwinkendorf
1801 Randolph Road SE
Albuquerque, NM 87111

Boeing Engineering & Const. Co.
Attn: Roger Gillette
P. O. Box 3707
Seattle, WA 98124

Burns & Roe, Inc. (2)
Attn: G. A. Fontana
800 Kinderkamack Road
Oradell, NJ 07649

Chevron Research (2)
Attn: John Cape
R. Creek
576 Standard Avenue
Richmond, CA 94802

Cyro Industries
697 Route 46
Clifton, NJ 07015

U. S. Dept. of Energy (2)
ALO
Attn: James Morley
Ethan Walker
P. O. Box 5400
Albuquerque, NM 87115

U. S. Dept. of Energy (8)
Div. of PV Energy Technologies
Attn: R. Annan
M. B. Prince
L. Herwig (5)
A. Scolaro
1000 Independence Ave. SW
Washington, DC 20585

Purdue University (2)
Attn: Richard Schwartz
Mark Lundstrom
Electrical Engineering Dept.
West Lafayette, IN 47907

Quantum Specialties
Attn: James E. Molle
163 Verde Circle
Rohnert Park, CA 94928

Research Triangle Institute
Attn: Mayrant Simons
Box 12194
Research Triangle Park, NC 27709

SERI (3)
Attn: Gene Blakeslee
Lee Cole
John Benner
1617 Cole Blvd.
Golden, CO 80401

SERI, Library (2)
1536 Cole Blvd., Bldg. #4
Golden, CO 80401

Southern Cal Edison
Attn: Spencer Carlisle
2244 Walnut Grove Ave.
Rosemead, CA 91770

Spectrolab
Attn: Brian Elm
12500 Gladstone Avenue
Sylmar, CA 91342

Spire (3)
Attn: S. Tobin
M. Nowlan
R. Little
Patriots Park
Bedford, MA 01730

Star Light Energy
Attn: J. Furber
1717 18th Street NW
Washington, DC 20009

Strategies Unlimited
201 San Antonio Circle
Suite 205
Mountain View, CA 94040

Solar Works
Attn: Paul Wilkins
Route 2, Box 274
Santa Fe, NM 87501

Thermo Electron
Attn: Ron Scharlack
45 First Avenue
Waltham, MA 02154

UNM/NMERI
Attn: G. Leigh
Campus Box 25
Albuquerque, NM 87131

Varian & Associates (20)
Attn: Peter Borden
N. Kaminar
611 Hansen Way K-219
Palo Alto, CA 94303

University of Wisconsin
Attn: Prof. J. D. Wiley
Dept. of Electrical Engineering
Madison, WI 53706

Wright Patterson AFB
Attn: Jack Geis
AFWAL/POOC
Wright Patterson AFB, OH

Wyle Labs (2)
Attn: Dave Christenson
George Meares
7800 Governors Drive West
Huntsville, AL 35807

E-Systems (2)
Attn: Mark O'Neill
A. J. McDanal
P. O. Box 226118
Dallas, TX 75266

General Electric Co.
Attn: Ron Hodge
P. O. Box 527
King of Prussia, PA 19406

International Rectifier
Attn: Harold Weinstein
235 Kansas Street
El Segundo, CA 91214

Intersol Power Corporation
Attn: John Sanders
7400 W. Radcliff Avenue
Littleton, CO 80123

Jet Propulsion Lab (3)
Attn: K. Shimada
R. Ferber
Solar Data Center
4800 Oak Grove Drive
Pasadena, CA 91109

Martin Marietta (4)
Attn: S. Broadbent
R. Hein
D. Hughes
J. Baumann
P. O. Box 179
Denver, CO 80201

Microwave Associates
Attn: Jonathon Chapple-Sokol
South Avenue MS-116
Burlington, MA 01803

McGraw Hill
607 Boylston St.
Boston, MA 02116

3M
Attn: Sanford Cobb
Industrial Optics
235 2D15
3M Center
St. Paul, MN 55144

Motorola
Attn: Keith Kingston
GED
8201 E. McDowell
Scottsdale, AZ 85252

NASA, HQ
Attn: John Loria
Code RET-1
Washington, DC 20546

New Shelter Home Magazine
9317 Shoshone
Albuquerque, NM 87111

Oak Ridge National Lab
Attn: Steve Kaplan
P. O. Box X
Oak Ridge, TN 37830

Oklahoma University
571 South University Blvd.
Norman, OK

Photowatt (2)
Attn: William Taylor
Mike Keeling
2414 W. 14th Street
Tempe, AZ 85281

Power Hybrids
Attn: Jeff Meyer
1742 Crenshaw Blvd.
Torrance, CA 90501

PRC
Attn: E. Stirewalt
5201 Leesburg Pike
Suite 400
Falls Church, VA 22070

1133 R. Chaffin
1133 J. Wiczer
1811 R. Assink
1822 J. Sweet
Attn: M. Moss
R. Pettit
1823 M. Chamberlain
1845 R. Eagan
2142 B. Rose
2146 M. Garner
2146 B. Hanson
2146 B. Nasby
2146 J. Rodriguez
2146 H. Weaver
9700 E. Beckner
9720 D. Schueler
9721 J. Banas
9721 H. Gerwin
9723 E. Burgess
9724 E. Boes
9724 D. Arvizu
9724 L. Beavis
9724 C. Chiang
9724 M. Edenburn
9724 D. King
9724 A. Maish
9724 M. Rios
9724 C. Stillwell
3141 L. J. Erickson (5)
3151 W. L. Garner (3)
3154-3 C. H. Dalin (25)
For DOE/TIC (Unlimited Release)
8214 M. A. Pound